T.R.
BOLU ABANT İZZET BAYSAL UNIVERSITY
INSTITUTE OF GRADUATE STUDIES

DIP COATING OF TUNGSTEN TRIOXIDE ON A STAINLESS STEEL

MASTER OF SCİENCE

MUSA MOHAMMED KABA

BOLU, OCAK - 2021

T.R.
BOLU ABANT İZZET BAYSAL UNIVERSITY
INSTITUTE OF GRADUATE STUDIES
Department of Chemıstry

DIP COATING OF TUNGSTEN TRIOXIDE ON A STAINLESS STEEL

YÜKSEK LİSANS TEZİ

MUSA MOHAMMED KABA

ACADEMIC SUPERVISOR
Prof. Dr. Izzet MORKAN
ACADEMIC CO-SUPERVISOR
Prof. Dr. Aivaras KAREIVA

BOLU, OCAK - 2021

APPROVAL OF THE THESIS

Dip-coating of tungsten trioxide on a stainless steel submitted by **Musa Mohammed KABA** and defended before the Examining Committe Members listed below in partial fulfillment of the requirements for the degree of **Master of Science** in **Department of Chemistry, Institute of Graduate Studies of Bolu Abant Izzet Baysal University in 6.01.2021** by

Examining Committee Members	**Signature**
Supervisor Prof. Dr. Izzet MORKAN Bolu Abant Izzet Baysal University	.....
Member Dr. Erhan BUDAK Bolu Abant Izzet Baysal University	.....
Member Doç. Dr. Abdulkadir ALLI Düzce University	.....

Prof. Dr. Osman GÖRÜR.....

Director of Instıtute of Graduate Studies

Dedication Page

I thank the almighty God for giving me such loving parents (Majula Darame and Fatumata Darame) for their enthusiasm for acquiring more knowledge.

Thanks and appreciation to all teachers, friends, and family members that help in their own ways to see me successfully completing my education up to this level.

During my studies, I encounter both good and bad times. I was able to overcome those difficult times due to your continuous courage & support, and I hope you continue those great efforts up to the next level of my academic career. I shall always try my best not to let you all down.

Indeed, I am very much grateful and will forever remember your kindness and impact every one of you play in order for me to become successful.

ETHICAL DECLARATION

In this thesis dissertation that was properly prepared according to the Thesis Writing Rules of Bolu Abant İzzet Baysal University of the Institute of Graduates Studies, I hereby declare that;

- All data, information, and documents presented in the thesis were obtained in accordance with the academic and ethical rules,
- All data, documents, assessments, and results were presented in accordance with the scientific ethical and moral rules,
- All works that were benefitted in the thesis were appropriately cited,
- No alteration was made in the data used,
- Study presented in this thesis is original,

Otherwise, I declare that I accept the loss of all my rights in case any contradiction that may arise against me.

_____

Musa Mohammed KABA

ABSTRACT

DIP COATING OF TUNGSTEN TRIOXIDE ON A STAINLESS STEEL
MSC THESIS
MUSA MOHAMMED KABA
BOLU ABANT IZZET BAYSAL UNIVERSITY
INSTITUTE OF GRADUATE STUDIES
DEPARTMENT OF CHEMISTRY
(SUPERVISOR: PROF. DR. IZZET MORKAN)
(CO-SUPERVISOR: PROF. DR. AIVARAS KAREIVA)
BOLU, JANUARY 2021

Thin films coating of molybdenum-doped tungsten trioxide (WO3-Mo) and tungsten trioxide (WO3) were produced from aqueous solutions on a stainless steel substrate using simple dip-coating technique and the 5^{th}, 10^{th}, and 15^{th} film layers analyzed were continuous and homogeneous. The crystallinity and morphology of the films produced on the stainless steel surface depended on the concentration of the polyvinyl alcohol (PVA) in the aqueous solution and the metal cation species. From the analysis of the FE-SEM, spike-like nanostructures were revealed from the construction of the WO3 dip-coated film surfaces. From the measured values of the static water contact angle on the coated steel film surfaces indicated that the WO3 film deposited can possess both hydrophobic and hydrophilic behavior, whereas WO3-Mo films displayed hydrophilic character. The surface of coated steel samples held a lubricating layer that is significantly better than the original stainless steel samples, exhibiting a foremost reduction in wear and friction. Base on these outstanding thermal, hydrophobic and hydrophilic properties of WO3 and WO3-Mo coated films along with simple dip-coating method suggest a very auspicious ability in industrial usage.

KEYWORDS: Wet-chemistry, X-ray diffraction, Contact angle, Thin films, Tungsten trioxide, Surface structure, Field-emission scanning electron microscopy.

ÖZET

PASLANMAZ ÇELIK ÜZERİNE DALDİRMA YOLUYLA TUNGSTEN TRİOKSİT KAPLAMA
YÜKSEK LISANS TEZI
MUSA MOHAMMED KABA
BOLU ABANT İZZET BAYSAL ÜNİVERSİTESİ
LİSANSÜSTÜ EĞİTİM ENSTİTÜSÜ
KİMYA ANABILIM DALI
(TEZ DANIŞMANI: PROF. DR. IZZET MORKAN)
(İKİNCİ DANIŞMAN: PROF. DR. AIVARAS KAREIVA)
BOLU, OCAK 2021

Molibden katkılı Tungsten trioksit (WO3-Mo) ve Tungsten trioksitin (WO3) ince filmleri sulu çözeltilerinden paslanmaz çelik üzerinde basit daldırma tekniği kullanılarak üretildi ve incelenen 5. 10. Ve 15. Film tabakaları sürekli ve homojendir. Paslanmaz çelik üzerinde üretilen filmlerin kristalliği ve morfolojisi sulu çözeltideki polivinil alkolün konsantrasyonu ve metal katyonun türüne bağlıdır. FE-SEM analizinden, desenli WO3 film yüzeylerinin başak benzeri nano yapılara sahip olduğu açığa çıktı. Çelik yüzey üzerine kaplanmış filmlerin ölçülen statik su temas açısı değerleri, WO3-Mo filmlerin hidrofilik davranış gösterirken WO3 filmlerin ise hem hidrofobik hem de hidrofilik yapıya sahip olabileceğini gösterdi. Kaplanmış çelik örneklerin yüzeyi, sürtünme ve aşınmada büyük düşüş sergileyerek orijinal çelik örneklerin yüzeyinden çok daha iyi kayar yüzeye sahipti. Basit daldırma yöntemiyle hazırlanan WO3-Mo ve WO3 kaplı filmlerin bu olağanüstü termal, hidrofobik ve hidrofilik özellikleri endüstriyel kullanıma olanak sağlar.

ANAHTAR KELİMELER: Islak kimya, İnce filmler, Tungsten trioksit, Yüzey yapısı, X ışını kırınımı, Alan emisyonlu taramalı elektron mikroskobu, Temas açısı.

TABLE OF CONTENTS

LIST OF FIGURES

Description **Page**

LIST OF TABLES

Page

LIST OF ABBREVIATIONS AND SYMBOLS

CA	: Contact angle
DSC	: Differential Scanning Calorimetry
DTG	: Derivative Thermogravimetry
EDTA	: Ethylenediaminetetraacetic acid
EDS/EDX	: Energy Dispersive X-Ray Spectroscopy
FE-SEM	: Field Emission Scanning Electron Microscopy
FT-IR	: Fourier-transform Infrared Spectroscopy
SEM	: Scanning Electron Microscopy
TG	: Thermogravimetry
XRD	: X-ray Diffraction
PVA	: Polyviyl alcohol
WCA	: Water Contact Angle
W_Mo_O	: Molybdenum-doped tungsten trioxide complex
WO3-Mo	: Molybdenum-doped tungsten trioxide
W_O	: Tungsten trioxide complex
WO3	: Tungsten (VI) oxide, WO_3
$W\_O_{(PVA)}$	: Complex of Tungsten trioxide with a higher amount of polyvinyl alcohol.

ACKNOWLEDGEMENTS

Special thanks and appreciation to my professors (Izzet Morkan and Aivaras Kareiva) for offering me the chance to expand my knowledge of research in the scientific research laboratory and for the characterization of the results at the Institute of Chemistry, Faculty of Chemistry and Geosciences, Vilnius University, Vilnius LT-03225, Lithuania. Also, gratitude to Dr. Edita Garskaite, Dr. Andrius Laurikenas and Dr. Aurelija Smalenskaite for technical assistance in difficulties encounter during research.

This is to acknowledge that this research had support from the Lithuanian Council of Research by a grant SEMAT (No. SEN-02/2016) of the National Research Programme "Healthy ageing". Also, not to forget the great relationship between the two universities (Vilnius University & the Bolu Abant Izzet Baysal University) that produced students/researchers in order to carry on this scientific research project.

Furthermore, not to forget the Ilim Yayma Vakfi who help me with a one-year scholarship to continue my studies and all those who help in making this successful.

1. INTRODUCTION

Metal oxides are part of the nanomaterials that are mostly accepted and broadly utilised as an active catalyst or supporting material [1] and having constituents that are very useful for smart devices and other advanced functional materials development [2]. In order to accomplish that (i.e., unlocking their full potential), nanostructuring has surfaced as the best tool. Many metal oxides in their bulk state generally are stable systems and robust with well-defined crystallography structures that demonstrate band gaps that are wide and reactivity that is low [3].

Stainless steel may be used in a range of fields for many other reasons like transportation and construction purposes [4–6]. The adhesion and acquisition of various organic and inorganic substances atop the surface of steel throughout its interaction with the environment can give rise to the growth of biofilm and corrosion of the material [7–9]. Over a long period of time, these activities lower the durability of the material and escalate the maintenance cost which has led numerous studies to be carried on in order to invent anti-wetting and anti-rust coatings with mechanical durability that is good. In the 1930s development of crucial materials that were used generally in the production of non-wetting slippery surfaces are polymers with low surface energy such as polytetrafluoroethylene (PTFE; commonly known as Teflon) and polydimethylsiloxane (PDMS; a common silicone rubber) [10]. In environments that are very harsh where the application of plastics is not possible the inorganic materials find use in inventing water-repellent coatings [11]. For example, metal oxides can adopt a very great extent number of structural geometries with an electronic structure that possesses the character of metal, semiconductor, or insulator.

Series of studies have been carried on about Tungsten (VI) oxide (WO3) for their chromism photo-catalysis and sensing capabilities, however, it also possesses other important properties and functionalities that much time have not been cater to in the past [2]. The stoichiometric of WO3 may be used as an

example of a metal oxide having a band gap of ~2.7 eV that permits the absorption of visible light reaching to 500 nm.

Many reports have shown that in acidic aqueous conditions it is thermodynamically stable and mechanic durability is also high [12-16]. Due to these physiochemical that allowed the investigation of WO3 films as a prospective material for the photocatalytic treatment of wastewater [17–19] and the antifouling coatings [20]. The co-operation of Mo ions in the WO3 medium that improves the antimicrobial properties has been studied [21,22]. In general, ceramics and metals tend to be water loving (i.e; hydrophilic), as these substances surfaces are well recognized to possess a great number of polar sites indebted to coordinative unsaturation [23,24]. Thus, another possible means of solid surface modifications to alter its wettability is the texturing of its surface. Such effects were substantiated for super-hydrophobic pure steel surfaces with steady contact angle (CA) having values of ~154° which were constructed using direct laser texturing by Ta et al. [25]. In addition, WO3 films that are highly textured and displayed wettability that is reversible between hydrophobicity and hydrophilicity were obtained by Gu and Tu [26]. It should also be noted that the solid hydrophobicity is intensified by the roughness of the surface, but the degree varies based on the shape of the surface [27]. For example, morphologies of the surface showed distinctive wettability of the nanostructured films of ZnO grown using the wet chemistry method demonstrated by Shaban et al. [28].

The techniques of deposition for WO3 films span solution based methods (sol-gel [29], electrochemical [20,30]), chemical vapour deposition (CVD) [31] to physical depositions in high vacuum (pulsed laser deposition (PLD) [32], and sputtering [13,14]),_however, every one of these technique proposes specific gains. The solution-based synthesis method to construct oxide films is notably flexible, for reason that it unlocks an amusing range of solvents, precursors, and organic-additives like wetting along with complexing agents to get morphologies that are desirable [33,34].

In many instances, in order to change as the amorphous film deposited into the crystalline film, a post-deposition heating step is needed. Hence, the

morphological and structural properties of the constructed film (i.e., microstructure & density) can further be acclimated base on the several thermal processing states applied.

In this experiment, an account is given on the synthesis route of a chemical solution-based to dip-coat WO3-Mo and WO3 thin films on stainless steel substrate wherein 12-molybdophosphoric acid hydrate and ammonium metatungstate hydrate used as metal precursors, ethylenediaminetetraacetic acid (EDTA) used as a complexing agent, and aqueous polyvinyl alcohol (PVA) solution used as a wetting agent in order to improve the substrate wettability. The classification of the morphology of the resulting films showed crack-free and uniform film formation. The WO3 films in contract to that of the WO3-Mo films displayed spike-like topographical nanoscale structures. The deposited films' properties of wettability were examined and ascertained that the films deposited wetting behavior were interrelated to the morphology of the surface. Furthermore, the dip-coated films tribological behavior was investigated and the obtained results showed greater mechanical durability from all coatings of WO3 film examinations that were accredited to the films' higher density [35].

2. AIM AND SCOPE OF THE STUDY

The aim and objectives of this research are to create a protective cover coating (of a steel-like material) that will help extend the life span of a steel-like material, reduce costs of repelling, prevent the problems encountered in sewage (wastewater treatment) after anaerobic digesters secrete phosphate and ammonium ions from waste material and other harmful substances. The coating cover should exhibit properties [of friction (or tribology), anti-microbial, thermal (heat resistance) &, etc.] that can prevent harmful substances from sticking to the surface of the steel and protect the original steel material.

In doing so, dip-coating is one of the most efficient ways to achieve that. The sol-gel (dip-coating sol) must have the properties mentioned above and other tests like XRD, SEM (scanning electron microscope), and other important examinations must be carried on to prove that the layers of the coats are strong enough to prevent those harms.

3. MATERIALS AND METHODS

Nano-powders or nanoparticles of tungsten oxide (WO3) is a multipurpose material with many advantages such as low cost of fabrication, antimicrobial properties, available in the form of nanofluids or faceted high surface area oxide particles revealing magnetism, and other forms are dispersed, transparent, coated (in the form of thin films) and the level of purity is high.

3.1 Properties Of WO3

Tungsten (W) is found in the transition metals and belongs to Period 6, Block D, while oxygen (O) is found in the nonmetal and belongs to Block P, Period 2 of the periodic table. The nanoparticles of Tungsten oxide have a yellowish appearance and the morphology is nearly spherical.

Table 1: Properties of Tungsten (VI) oxide

Chemical Properties	
Chemical symbol, IUPAC Name / Other Names	WO_3, Tungsten trioxide / Tungsten (VI) oxide, Tungstic anhydride
Group	Tungsten: 6, Oxygen: 16
Electronic Configuration	Tungsten: [Xe] $4f^{14}$ $5d^4$ $6s^2$, Oxygen: [He] $2s^2$ $2p^4$
Chemical Composition	
Element	**Percent Content (%)**
Tungsten	79.29
Oxygen	20.69

Thermal Properties	
Properties	**Values**
Melting Point	1473 °C
Boiling Point	1700 °C
Physical Properties	
Properties	**Values**
Density	7.16 g/cm3
Molar Mass	231.84 g/mol
Water Solubility	Insoluble
Main Hazard / Flash point	Irrıtant / Non-Flammable

3.2 A Brief Explanation Of The Sol-Gel And Dip-Coating Method.

The sol-gel process is useful for the production of materials that are solid from small molecules and the process includes the transformation of monomers into a colloidal solution (sol) that serves as the precursor for an integrated network (or gel) of either polymers network or discrete particles [36]. For short, it is an oxide network establishment within polycondensation reactions of a precursor molecule in a specific liquid depending on the needs. In the 1960s, the need for a new synthesis method in the nuclear industries led to the development of this method. Sol-gel synthesis consisted of dissolving a compound in a liquid with the notion of bringing it back as a solid in a well-coordinated form and controlled stoichiometry, homogeneously small particle sizes.

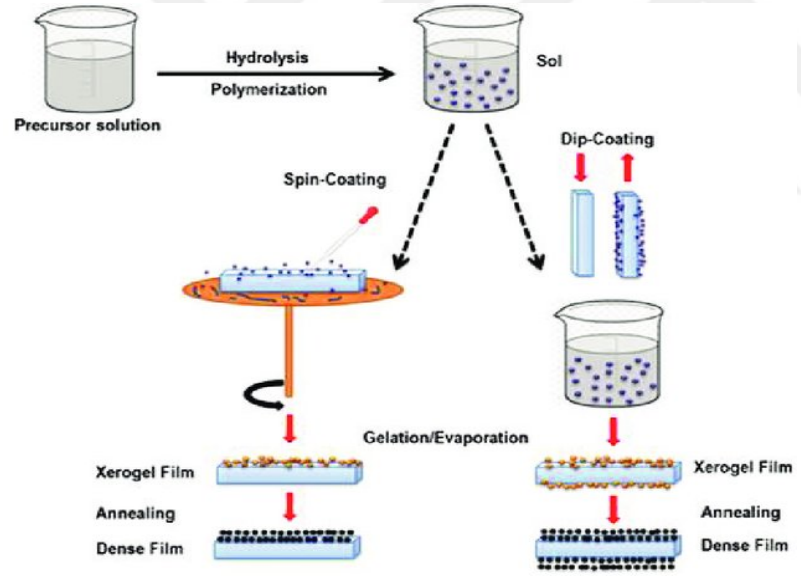

Fig. 1: Diagram briefly showing the sol-gel and thin film processing [37].

The Dip-coating technique is a wet chemical approach that involves the creation of a thin film from a chemical solution in order to protect the specific material(s) from certain harm(s) and also prolong the lifespan, and reduce the financial burden of the material. The dip-coating method is more famous than that of spin coating and is one of the oldest among the other wet chemical thin film coatings. It is also a simple method but attention needs to be given to the

redrawing speed. It is done mainly in three steps under controlled temperature and pressure:

i) the substrate material is immersed in the chemical aqueous sol/solution and dwells in it for a period of time,

ii) the substrate material is redrawn from the chemical sol/solution with a low redrawing speed wherein excess liquid is drained from it, and

iii) the evaporation of the solvent from the fluid during the deposition step which creates a thin film. The substrate is further dry/heated to improve the thin film layer.

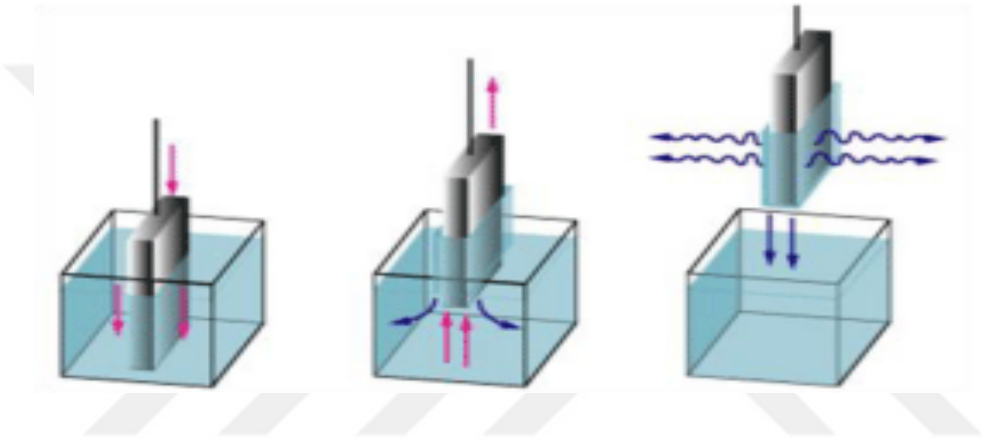

Fig. 2: Dip-coating process [38].

3.3 Compounds Used With Tungsten Oxide (WO3) In The Sol-Gel

Ethylenediaminetetraacetic acid (EDTA): a complexing agent that complexes the metal ion to form a smooth surface.

Polyvinyl alcohol (PVA, 1.2%): used as a wetting agent (i.e., for sol-gel formation).

Ammonium hydroxide (NH_4OH): used as EDTA deprotonating agent (EDTA + $4NH_4OH \xrightarrow{t°C} EDTA^{4-} + 4NH^{4+}$).

12-molybdophosphoric acid hydrate ($H_7[P(Mo_2O_7)_6]\cdot xH_2O$: a source of molybdate (Mo^{6+}).

3.4 EXPERIMENTAL SECTION

3.4.1 W_O, W_Mo_O And W_O$_{(PVA)}$ Sols, Gels, And Powders Preparation

In preparing the W_O-sol, 0.876 g (2.8·10−4 mol) ammonium metatungstate hydrate ($(NH_4)_6H_2W_{12}O_{40}\cdot xH_2O$, >85% WO3 basis (gravimetric), Aldrich) was firstly dissolved in a complexing mixture of ethylenediaminetetraacetic-acid (EDTA) (1.50 g, 0.009 mol), with 35 mL of distilled water. Few drops of NH_3 (conc.) solution was added to increase the pH and the mixture was stirred for 10 min on a magnetic stirrer. After stirring 50 mL of 1.2% aqueous polyvinyl alcohol (PVA) as a wetting agent was added in order to improve the final sol to the steel substrate.

W_Mo_O sol was prepared similarly (like W_O-sol) but with the addition of 0.186 g (0.9·10−4 mol) 12-molybdophosphoric acid hydrate ($H_7[P(Mo_2O_7)_6]\cdot xH_2O$, ACS, Alfa Aesar). Preparation of film from the same solution of W_O but with higher among of 1.2%PVA (i.e. 100mL PVA used). The labelings were done as follows: W_O, W_Mo_O, and W_O$_{(PVA)}$. By drying samples at 120°C with the rate of heating of 60°C/h for 24 h in an oven enable us to determine the volume of water crystallized in the precursor materials using the gravimetric analysis. The estimated percentage of weight loss after the evaporation of absorbed water was about 11% for the $(NH_4)_6H_2W_{12}O_{40}\cdot xH_2O$ and 13% for the $H_7[P(Mo_2O_7)_6]\cdot xH_2O$. Some portion of the W_O, W_O$_{(PVA)}$, and W_Mo_O sols prepared were evaporated at 65 °C in order to get inorganic-organic gels and then dry at 100 °C for 28 h. The gels were ground using mortar and pestle and then calcined at 650 °C for 5 h at a heating rate of 60°/ h. The quantitative analysis of the W and Mo elements percentage was done using Perkin Elmer Optima 7000 DV inductively coupled plasma optical emission spectrometer (ICP-OES) and was ascertained to be 87% for W and 65% for Mo.

3.4.2 Production Of Films From The Sols Prepared By The Dip-Coating Technique.

Stainless steel samples for dip-coating were prepared by sonicating them three and two times with acetone and isopropanol accordingly as a means to clean the surface of the steel before dip-coating. W_O, $W\_O_{(PVA)}$ as well as W_Mo_O sols were dip-coated (i.e. instrument KSV D, KSV Instruments Ltd.) on the stainless steel samples using immersion speed of 85.7mm/min, holding time (in solution): 10sec, holding time (after immersion in solution): 30sec, speed (after immersion): 40mm/min. The two speeds are different because at 85mm/min the steel is emerging in the sol in its dry form and at the speed of 40mm/min it is coming out of the solution which is lower than the immersion speed as a way to prevent the liquid from dropping off the steel. All film layers were dip-coated by a single immersion route and after each layer, the steel samples were calcined for five hours in a furnace at 650°C (heating rate 1 °C/min, holding samples at 650°C for 2-hours), as a means to burn all the organic parts and leave the inorganic part (which consists of WO3 & Mo) on the stainless steel.

3.4.3 Characterization Of Results

The morphology (i.e., elemental composition along with thickness) of the film layers was analyzed with field emission-scanning electron microscopy (FE-SEM, SU70, Hitachi) compacted with the Energy dispersive x-ray spectrometer (EDS) along with INCA software (Oxford Instruments). Secondary electron (SE) imaging mode was used to examine the sample film layers. Evaluation of the sintering temperature was done with the analysis of thermograph (TG) with the differential scanning calorimetry (DSC) (Netzch, STA 449C) of the gels reaching 800 °C in the air (at 10°/min rate of heating). The electron beam acceleration voltage was 5 kV for SEM and 20 kV for EDS analysis. The X-ray accusation time used to get the EDS spectra was 60 s. X-ray diffraction (XRD, MiniFlex II, Rigaku, Cu-Kα radiation, λ=0.1542 nm, 100 mA, 40 kV, 2θ=20–70°) was used to examine the structure of powders, films, and the phase purity.

Scherrer's equation ($dXRD=K\lambda/\beta \cos \theta$) was used to predict the WO3 powder samples average crystallite size, operating at half maximum & full-width of the (120), (200), (020) as well as the (002) reflections. Fourier transform infrared spectrometer (Frontier FT-IR, Perkin Elmer,(ZnSe ATR crystal, Liquid-nitrogen-cooled mercury cadmium telluride (MCT) detector), 4000–500 cm−1) was used to record the powder samples and dried gel infrared spectra. Also, the surfaces of the deposited film layers infrared spectra were noted in reflectance geometry by Thermo Scientific Nicolet iZ10 spectrometer in atmospheric air.

4. RESULTS AND DISCUSSION

4.1 Evaluation Of The Calcination Temperature

The dried gels of W_O and W_Mo_O calcination temperature were examined by performing thermal (TG/DSC) analysis. The W_O and W_Mo_O gels TG/DSC and DTG curves are shown in Fig. 3. Firstly, approximately 1.5 % of W_O gels' weight is lost at a temperature up to 100 °C which is allocated to the evaporation of water adsorbed. At 200–300 °C, the second and third weight losses observed were 13.5%, and 15% are traced to twofold endothermic reactions (DSC curve, maxima at 275 °C & 207 °C). In these temperature ranges, the initial precursor gel decomposition and organic fragments evolution occurred and mainly the loss of absorbed water molecules can be assigned to these processes.

The weight that was gradual loss next is approximately 20% allocated to organic matrix decomposition is perceived at temperatures reaching 550 °C not having a noteworthy change in the DSC curve (DTG maxima at 475 °C and 360 °C). The analyses of Ramana et al. showed that at the temperature of above 300°C, the promotion of WO3 crystalline from amorphous W_O film crystallization occurred [39]. In addition, at temperatures above 350 °C, a report has been given that WO3 phase transformation arises and throughout calcination WO3 crystallographic symmetry changes in the following sequence: monoclinic (ε-WO3) – triclinic (δ-WO3) – monoclinic (γ-WO3) – orthorhombic (β-WO3) – tetragonal (α-WO3) [39–41]. The DSC curve has some changes that may also be due to these transitions.

The final important weight loss of about 17% and simultaneously high exothermic process (at 604 °C, maximum broad peak) is noticed at temperatures up to 630 °C which can be allocated to the last elimination of the species that are organic and still existing in the WO3 material. Related thermal conduct was detected for the W_Mo_O gel however, in comparison to the W_O gel, the DSC curve for the W_Mo_O gel appeared at the lower temperatures. Around the scope of 200°C to 300°C one can notice two endothermic reactions emerging with the maxima positioned at 258 °C and 202 °C (DSC curve), and at the temperatures up

to 538 °C a high exothermic process occurred, while at the temperatures up to 600°C the last weight loss was acquired. From these observations, we can tell that W_Mo_O gel sintering temperature is around 65 °C lower compare to the W_O gel and very similar behavior was exhibited by $W\_O_{(PVA)}$ gel.

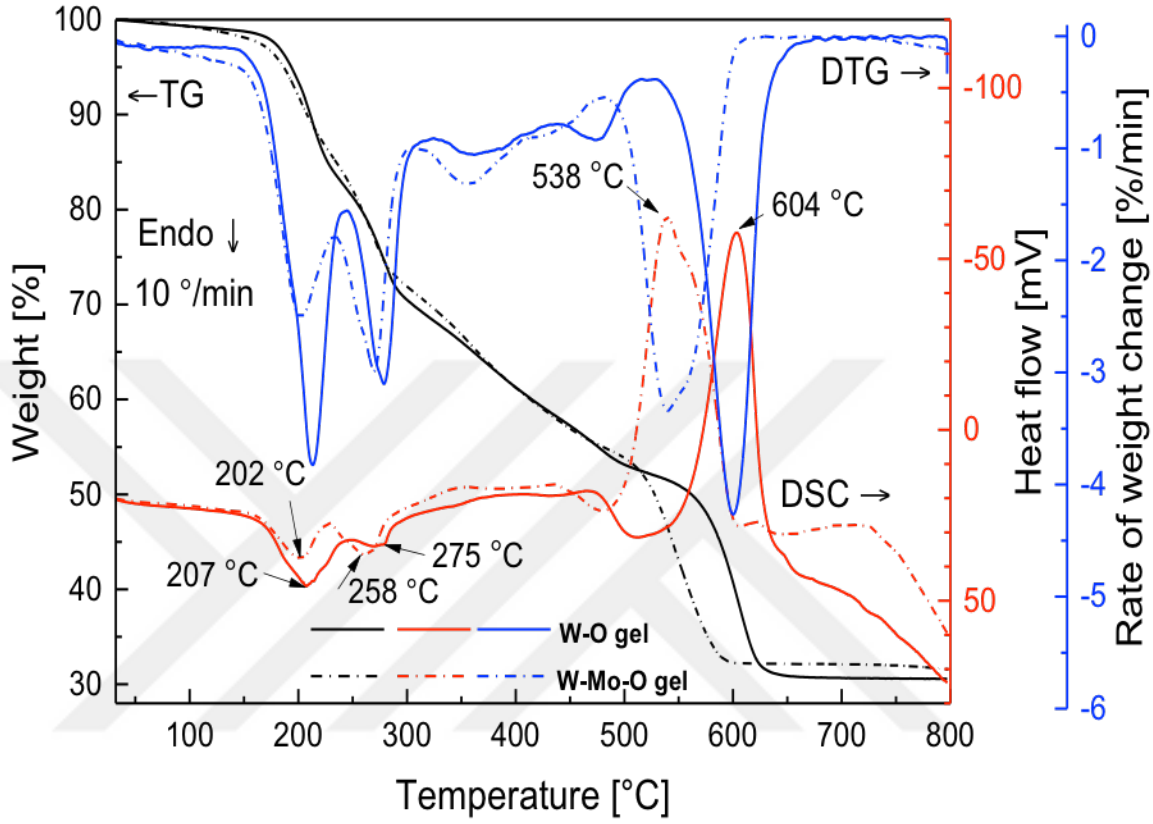

Fig. 3: The DTG and TG/DSC curves of W_Mo_O along with W_O gels.

4.2 Analysis Of The Morphology And Chemical Composition

4.2.1 Review Of The Coated Layers' Growth & Homogeneity Of the SEM Images Results At Different Micrometers.

As we claimed that the dip-coating method is one of the best and popular methods used to obtain good coatings, we will take a close look at the results obtained from this experiment in terms of homogeneity and layer growth. Also to note that when the layers are not homogeneously congested to each other, bacterial or other harms may find it way in the space between and gradually may cause serious harm over a period of time. In Fig.4 SEM images (from the lees deep boundaries) of the 5th coated film layers of W_Mo_O, W_O, along with

$W\_O_{(PVA)}$ annealed at 650C compared with the uncoated steel sample at 5 and 50 micrometers.

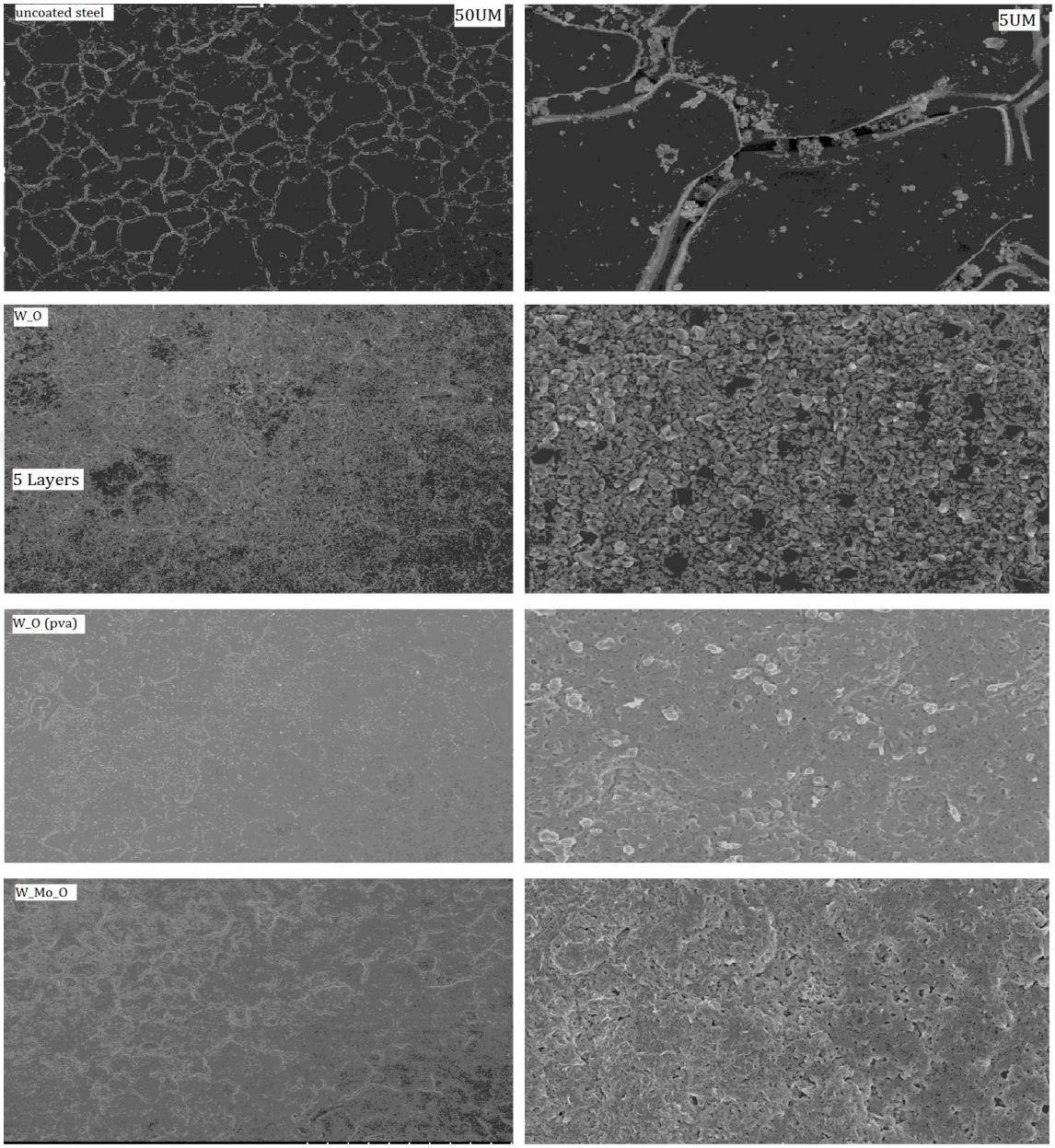

Fig. 4: 5 & 50 micrometers SEM images (of the 5th layer) from the smallest boundaries of the steel along with uncoated steel.

We can observe from this figure that the 5th layers were covering areas (of the stainless steel sample) that have less deep boundaries which tell us that the number of coats to be coated also depends on the holes or boundaries on the sample to be coated. It is also clearly shown from the five and one micrometers

SEM images that the 10th coated layer has improved greatly compare with the 5th coated layer Fig. 5.

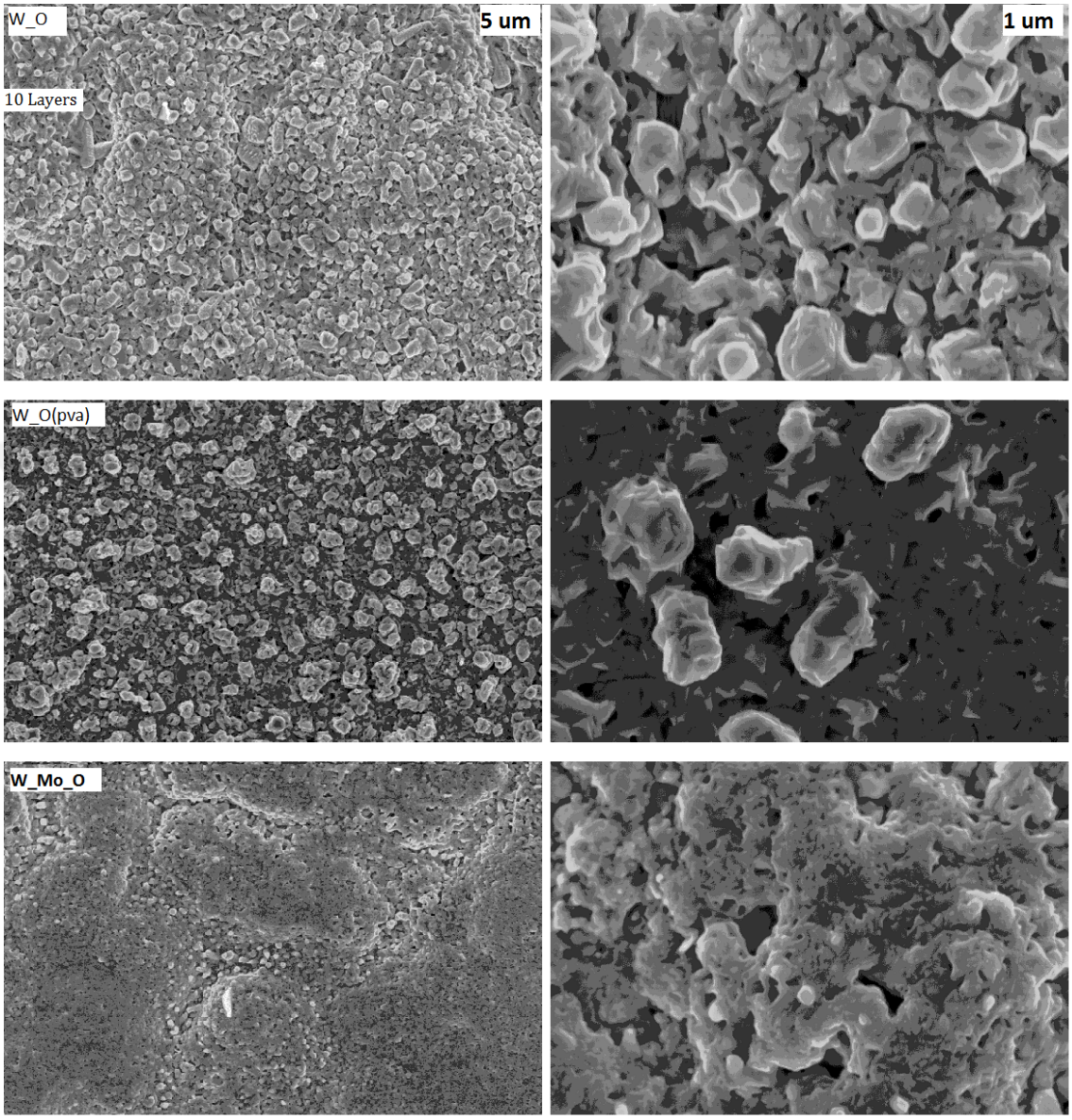

Fig. 5: The five & one micrometers SEM images of the 10th coated film layers.

Our fifteen film layers were able to cover the deepest holes and boundaries present on the stainless steel surfaces but yet still not sufficient to stop all harm from the surface of the stainless steel. In comparing our 15th final film layer with the uncoated steel substrate (Fig. 6), one can observe the great change in the size of the boundaries (from larger to lower) and the congestion and homogeneity of the coats are taken into consideration. All the three various samples coated show

gradual improvement of layers and as well as the uniqueness of coats from the dip-coating method.

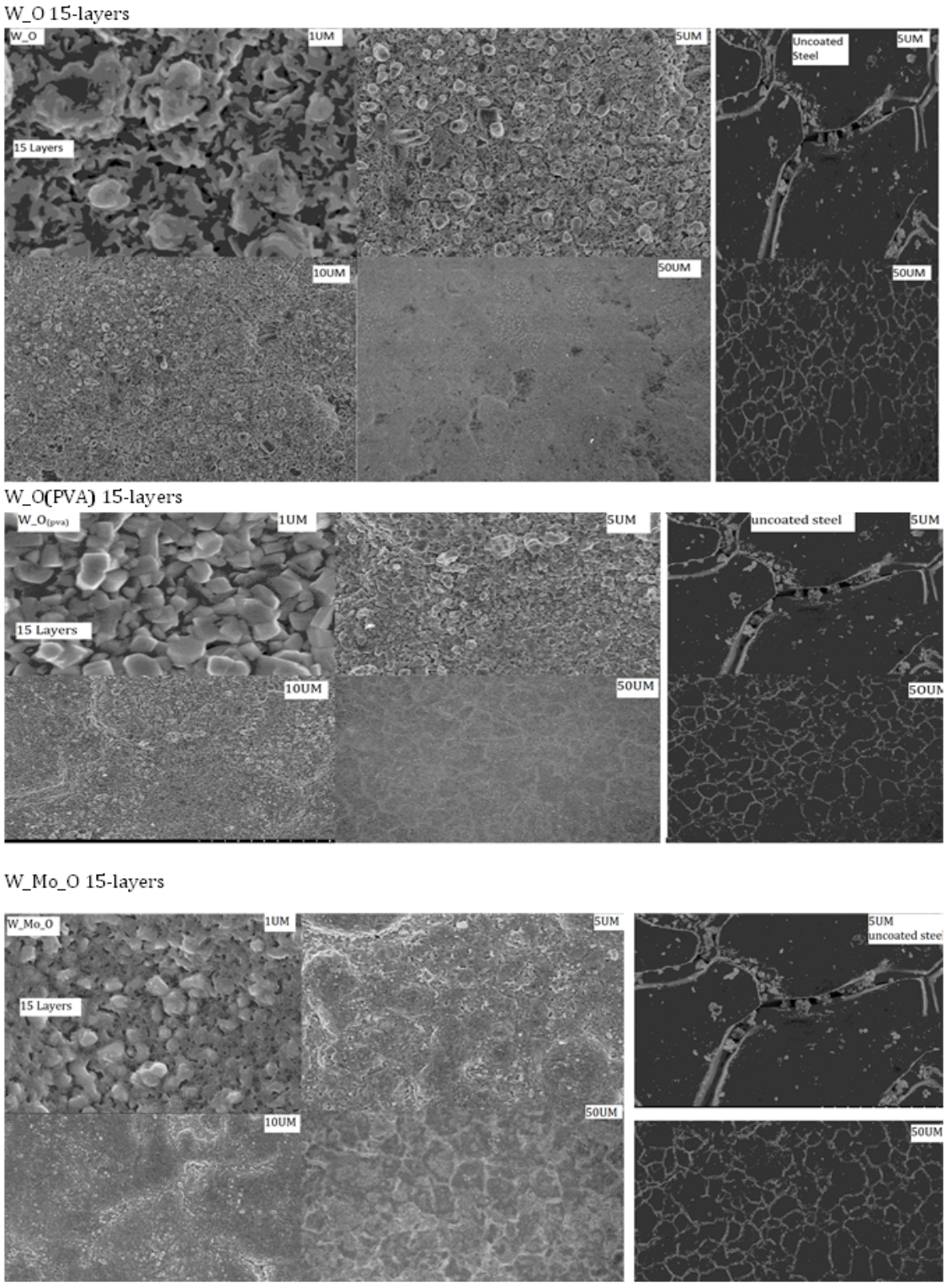

Fig. 6: SEM images of 15th coated layers (from all samples) compared with uncoated steel in various micrometers.

4.2.2 Justification Of The EDS Along With SEM Results Obtained

The X-ray and SEM of the 5th, 10th, and 15th film layers were analyzed. FE-SEM SE micrographs images of the W_Mo_O along with W_O (5th & 15th) film layers calcined at 650°C are displayed in Fig. 7 which showed the films uniformity and crack free. These images displayed that WO3 films (Fig. 7(a) & (b)) have a nanoscale spike-like structures with an approximately 350nm average diameter as well as spherical particles consisting of relatively small size nanostructures. From the image in Fig. 7 (c), where molybdenum ions are included in the complex system resulted in smoother surfaces than the pure W_O film.

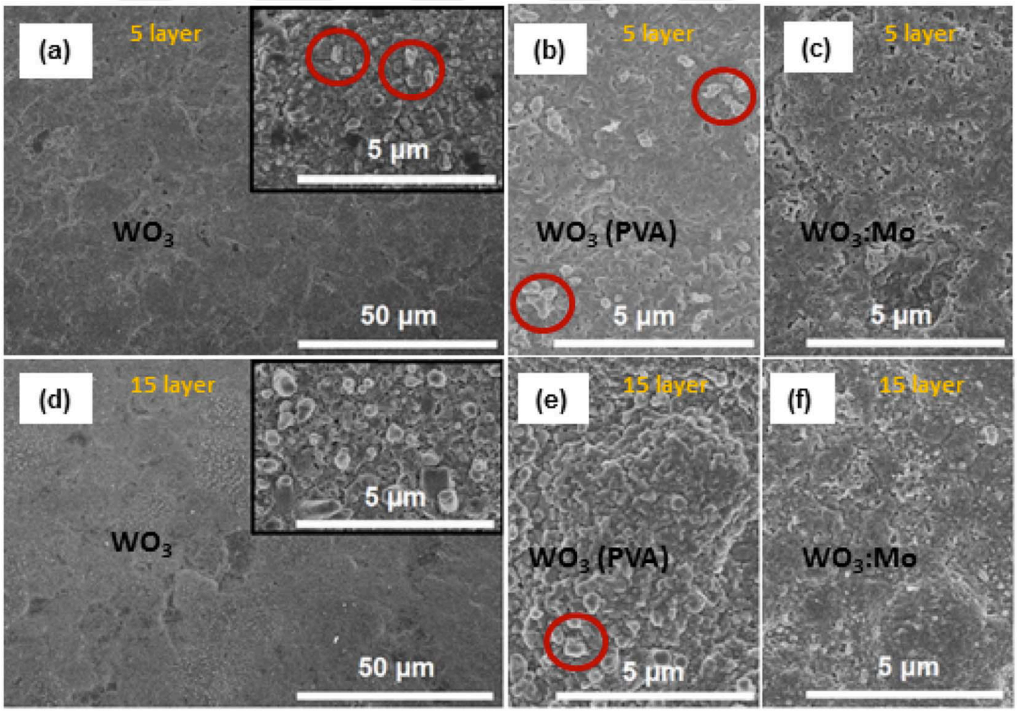

Fig. 7: FE-SEM micrographical images of the 5th & 15th layer ((a), (d)) W_O, ((b), (e)) $W\_O_{(PVA)}$ & ((c), (f)) W_Mo_O films calcined for 5 h at 650 °C .

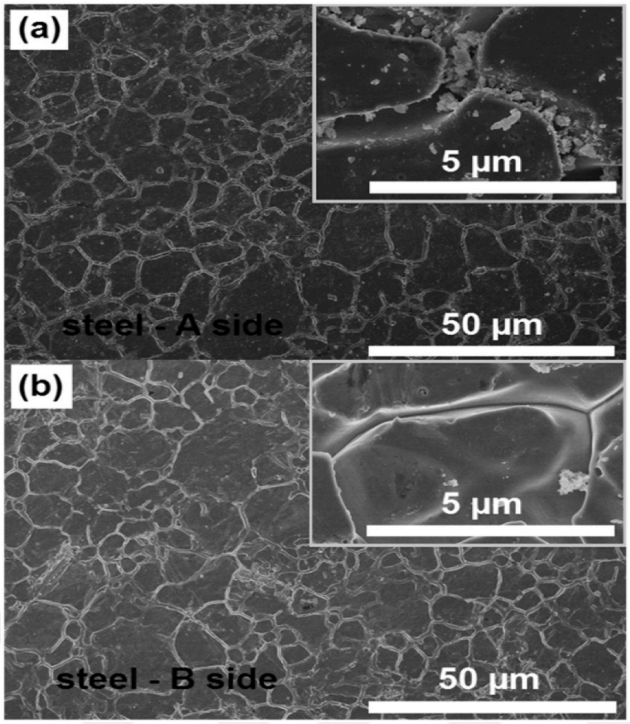

Fig. 8: FE-SEM micrographic images of the stainless steel substrate (a) upper-surface (A-side) and (b) lower-surface (B-side) (films produced on the upper-surface were examined).

The 10th film layer had similar morphologies as the previous and slightly more pronounce topographical features, which can be seen in Fig. 9. Among all the coated layers, the 15th film layers were observed and proven to have the best surface nanostructures (Fig. 7(d), (e) & (f)). Base on the results obtained, it is clearly understood that the surface is intensely improved or troubled by the number of film layers deposited and the composition of the sol. The results also showed how smooth the stainless steel surfaces have improved in comparison to the uncoated steel substrate (Fig. 8) (i.e. no sharp edges shown and evenly coating of grain boundaries Fig. 7).

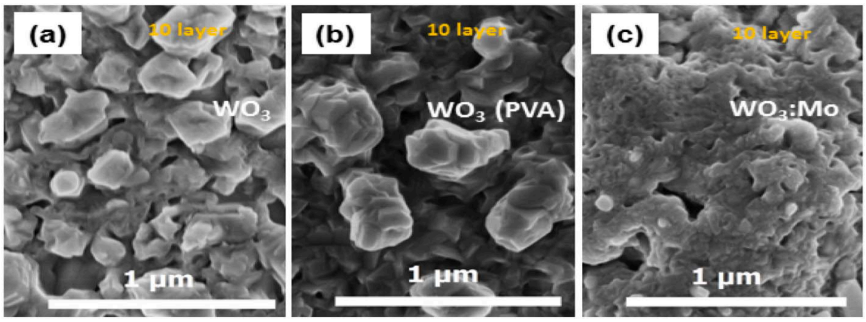

Fig. 9: FE-SEM micrographic images of 10th layer (a) W_O, (b) W_O$_{(PVA)}$ & (c) W_Mo_O films calcined at 650 °C for 5 h.

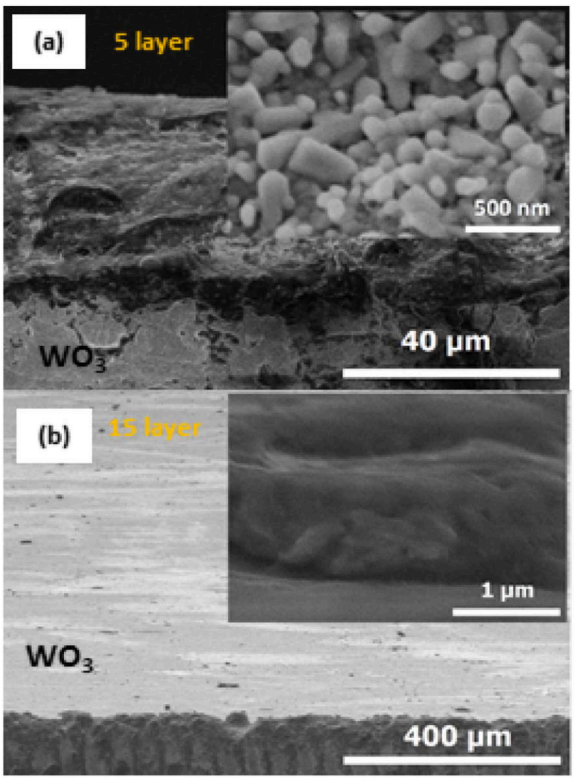

Fig. 10: Cross-sectional FE-SEM micrographic images of (a) 5th layer & (b) 15th layer W_O films calcined at 650 °C for 5 h; (a) inset shows the polycrystalline film microstructure and (b) inset presents W_O film from the coating center.

The cross-section FE-SEM micrographic images of the W_O films clearly showed the homogeneity and compactness of the film with no visible cracks (Fig. 10), and the size of the particle in the range of 50 to 200nm (Fig. 10(a) inset). The 15th film layer thickness was examined to be ranging from 1 to 1.5 µm (Fig. 10(b) inset), which indicates that a single film layer having an average thickness of

approximately 125nm is obtained from each coat in this method. Investigation of the W_$O_{(PVA)}$ film cross section revealed a slightly high range of porosity which can be because of the higher amount of PVA present in the specific sol and also from the released gases that increased throughout the heating process. The homogeneity, larger organic molecules, and polymeric effect found in the film structure were elaborated on by Grande et al. [34].

The resulting materials composition was examined with an EDS (Energy Dispersive X-Ray Spectroscopy) analysis on the 5th and 15th film layers. Images of the FE SEM and spectra of the EDS analysis of the W_Mo_O along with the W_O films are revealed in Fig. 11.

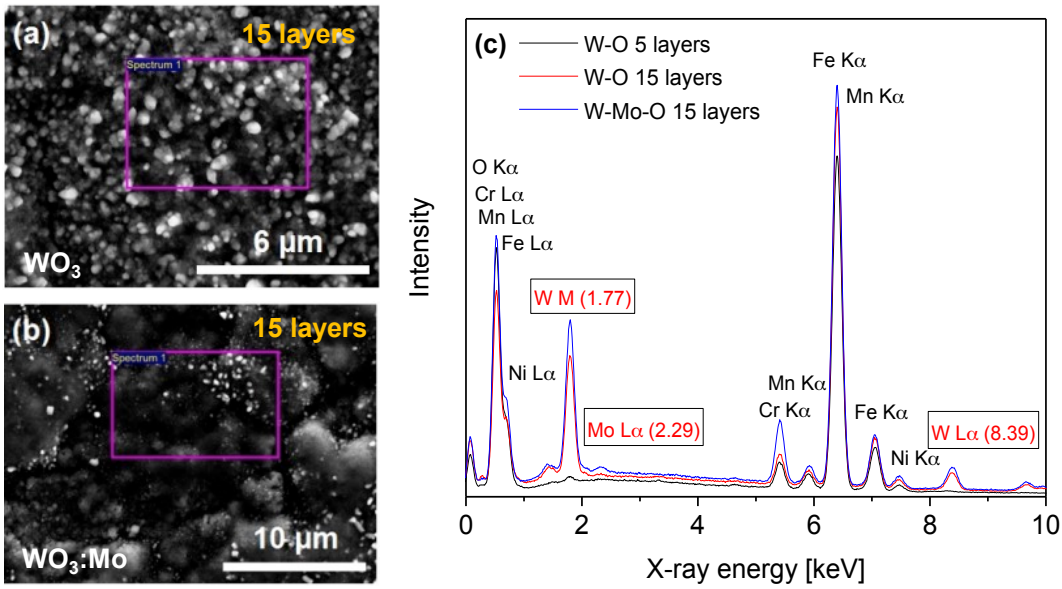

Fig. 11: FE-SEM micrographic images (places marked indicate the surface region scanned) along with the EDS spectrum of W_O & W_Mo_O films.

In the EDS spectrum, lines from elements such as Fe, Mn, W, Cr, Ni, C, Mo, and O were found which indicate that the stainless steel sample elements can be discovered even after the 15th layer coats and also show that fairly thin films were coated. The average percent atomic ratio of the elements (O: Cr: Mn : Fe : Ni: (Mo) : W) are: 54.94 : 1.79 : 0.98 : 36.67 : 1.27 : 4.36 and 50.60 : 6.65 : 0.78 : 36.16 : 2.14 : (0.37) : 3.31 for the W_O and W_Mo_O coated films, accordingly.

Similar spectral features were displayed for other samples that were prepared from the same sol composition. Evenly distributions of Mo, as well as W inside the films deposited, were revealed by the EDS elemental mapping.

4.3 Evaluation Of The Phase Purity And Crystal Structure

The W_Mo_O along with W_O 5th film layer X-ray diffraction (XRD) patterns are displayed in Fig. 12 and can be observed that the W_O and W_Mo_O films patterns produced Bragg reflections that are relevantly weak at 2θ=55.12°, 40.81°, 36.27°, 34.80° and 24.34°that were allocated to the (420), (222), (122), (202), and (002) diffraction peaks of WO3 (JCPDS no. 43-1035, monoclinic, space group P21/n(14)) phase [42,43].

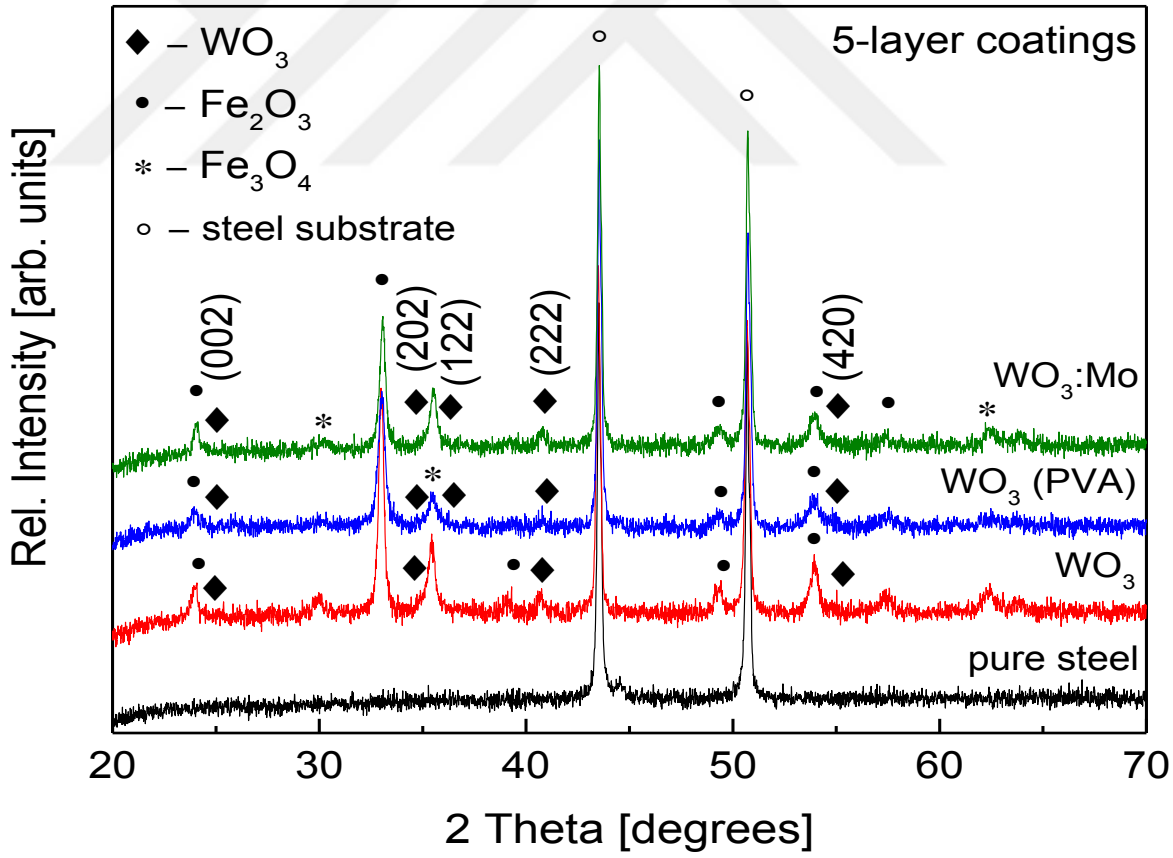

Fig. 12: The XRD patterns of the 5th coated layer of W_Mo_O, W_O, & $W\_O_{(PVA)}$ as well as the pure uncoated steel substrate calcined for 5 h at 650 °C.

This result implies that the coated films at this temperature (650 °C) are solid that is crystalline. Diffraction peaks that are sharply resolved arising from magnetite (Fe_3O_4) (JCPDS no. 96-901-0940) and hematite (Fe_2O_3) (JCPDS no. 96-900-9783) phases were also spotted signifying the thinness of the deposited films. In addition, it reveals that these processing and thermal treatments give rise to the transformations of phase in the microstructure of the stainless steel substrate. These modifications might further be utilized for the purpose of obtaining a combination of attractive different mechanical and physical properties [41,44].

Fig. 13 shows the XRD patterns of W_Mo_O and W_O coated 15^{th} film layer, calcined at 650 °C with higher intensity of diffraction peaks, while Fig. 14 reveals the XRD patterns of W_O powder calcined for 5 hours at 650 °C in order to verify the phase composition. In the diffraction pattern, reflections that are very important were attained at 2θ=22.9°, 23.5°, 24.4°, 26.5°, 28.6°, 33.2°, 34.0°, 35.4°, 41.5°, 47.0°, 48.2°, and 49.9°, which were allocated to the (002), (020), (200), (120), (112), (022), (202), (220), (122), (222), (004), (040) and (140) diffraction peaks of W_O polycrystalline phase and marginally elevated background shown in the XRD pattern is because of the amorphous nature of the sample holder) [42,43,45]. As previously stated that numerous distinctive crystal structures (tetragonal, orthorhombic, triclinic, and monoclinic) can be adopted by WO3, the three different peaks in the $22° < 2\theta < 25°$ range assure the crystallization of the WO3 monoclinic phase [41,46–49].

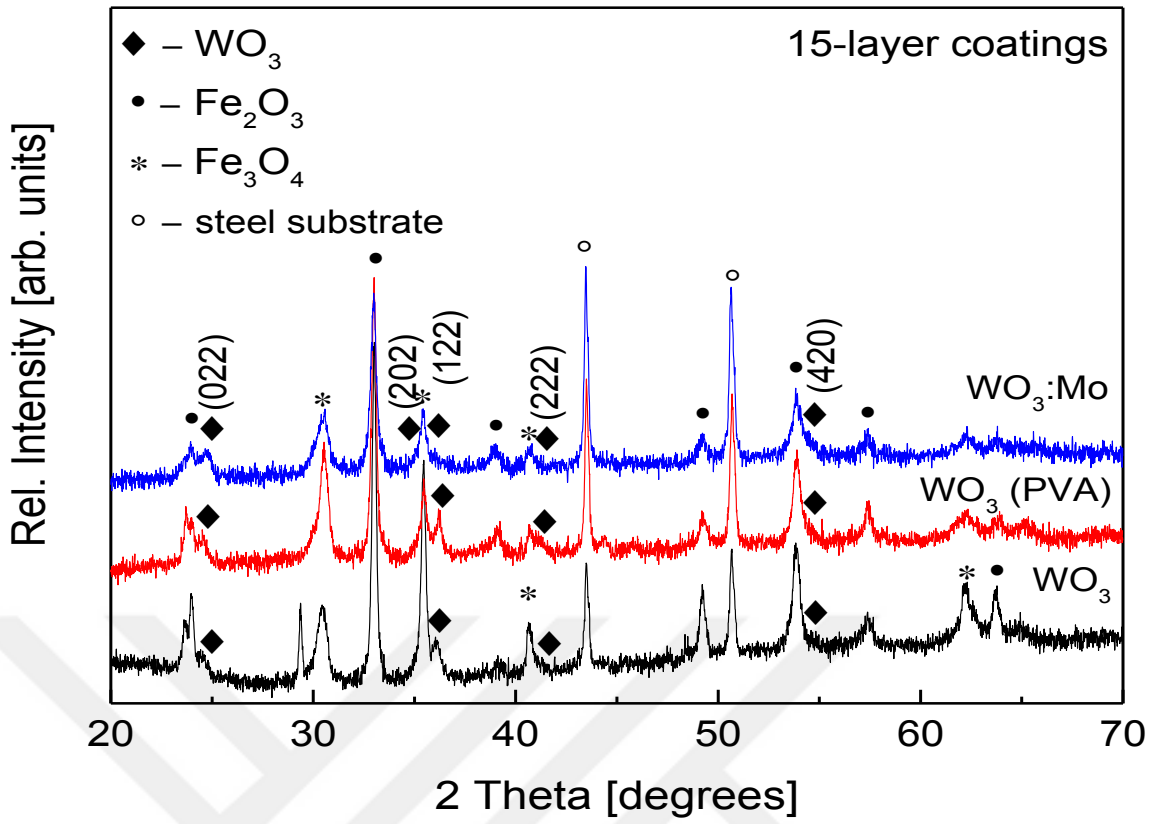

Fig. 13: XRD patterns of pure steel substrate and 15th layer W_Mo_O, W_O along with $W\_O_{(PVA)}$ coatings calcined for 5 h at 650 °C.

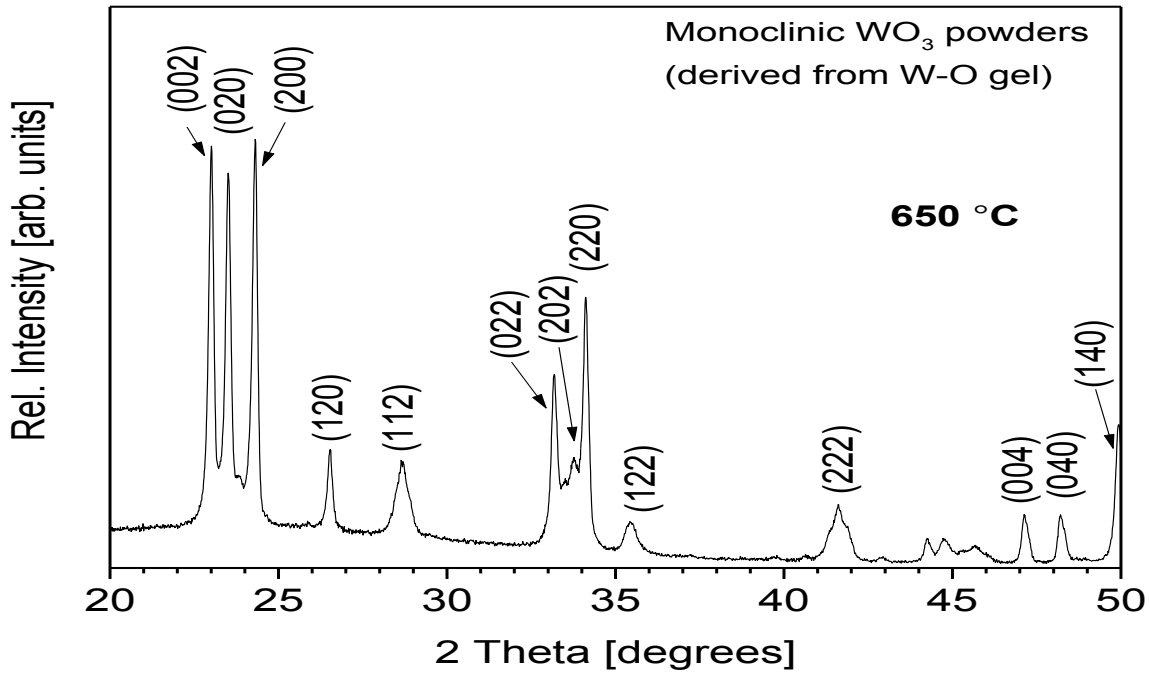

Fig. 14: W_O gel powders XRD diffraction pattern calcined at 650 °C displaying the crystalline monoclinic WO3 formation.

The powder crystallite (calcined at 650°C) average size was found to be 70.4 nm which indicates the corresponding size of the produced films crystallite on the steel. It is also in line with the FE-SEM examination (Fig. 10(a) inset) displaying that crystallite size (measured from the XRD patterns line broadening) is smaller in comparison to the particle's primary sizes determined by SEM analysis. It is clearly understood from the results that few crystallites made up a single particle.

4.4 FT-IR Spectroscopic Analysis

The 15th coated film layers of the various tungsten trioxides calcined at 650°C FT-IR reflectance spectra are displayed in Fig. 15 and the formation of the oxide layer can be found below the 1000 cm−1 region denoting the existence of metal-oxygen W-O-W and–W =O bonds [29,50]. The broadband spectrum of WO3 (around 2200-1400 cm−1) can be accredited to the gas-phase and adsorbed atmospheric water that is traced in the areas between 1400-1700 cm−1, and 3000–3600cm−1.

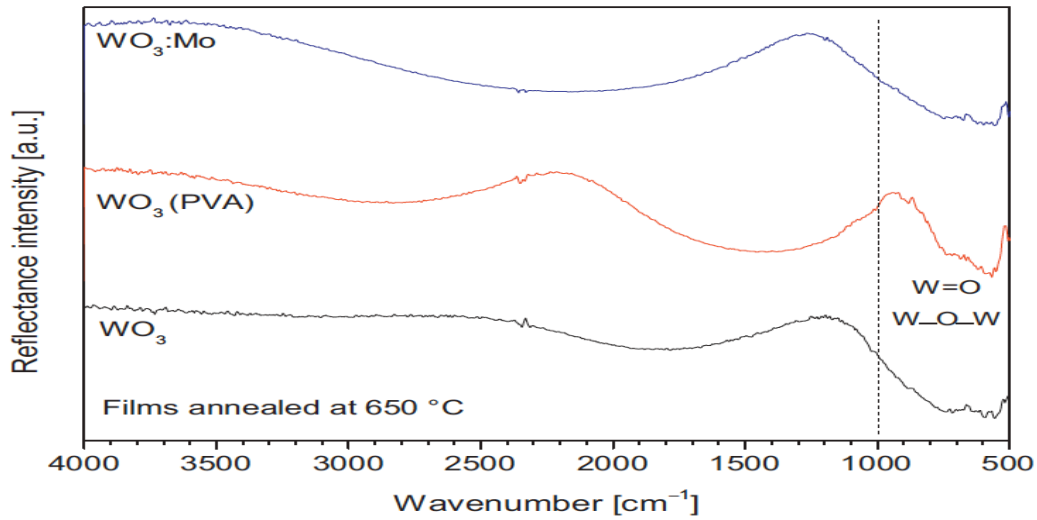

Fig. 15. FT-IR spectra of the 15th coated film layer of W_Mo_O, W_O, along with W_O$_{(PVA)}$ coatings calcined at 650 °C.

It is known that interferences in the spectra are caused by varying amounts of CO_2 and atmospheric water in the path of the light and the spectral band interpretation may be obstructed due to it [51]. It is observed that the W_$O_{(PVA)}$ film spectrum exhibit two bands that are broad around 3100–2500 cm−1 and 2000–1000 cm−1 while the W_Mo_O film spectrum have broadband around 1600 to 2700 cm−1, and they can be related to the CO_2 vibrations and molecules of water overlapping vibrations [52]. In predicting that metal oxide surface comprises OH & H_2O groups which might further affect the deposited films surface behavior resulting from exposure to the atmosphere is uncertain and other researchers have also propounded about such effects [54–55]. The dried W-O gel (at 100°C) as well as WO3 powders (calcined at 650°C) FT-IR spectra were also examined due to the comparatively weak reflectance of the W_O & W_Mo_O coatings (Fig. 16).

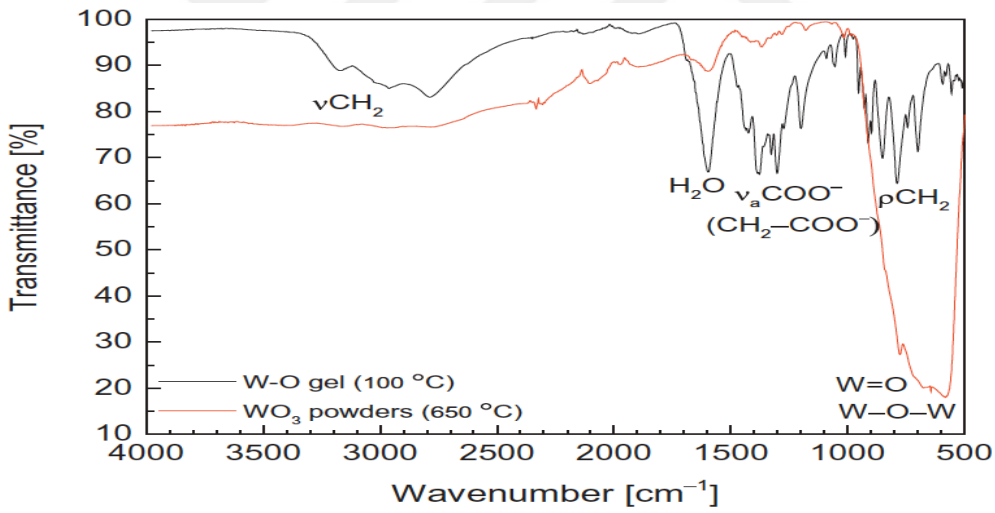

Fig. 16. FT-IR spectra analysis of the WO3 powders calcined at 650 °C and W-O gel dried at 100 °C.

From the W-O gel FT-IR spectrum analysis, it is certain that the bands display in the region around 3200 to 2600 cm−1 can be accredited to the stretching frequencies of the ν(CH2) (from the EDTA) [29,56,57] and the band approximately around 1600 cm−1 can be allocated to the bending mode of H2O [58]. The stretching vibrations of the ν(COO−) band are found in the region around 1450 to 1300 cm−1 while the band about 720 cm−1 in the low-frequency region can be assigned to the rocking vibrations of ν(CH2) [56]. The WO3

powder (annealed at 650 C) possessed spectral features that are different. In the region between 500 to 900 cm−1, broadband is observed with two maxima that are poorly resolved (at 582 and 672 cm−1) and the existence of W-O-W and W=O bonds were noted at 778 cm−1from a small shoulder. Similar WO3 films spectrum (produced from the sol-gel synthesis method) was observed by J. Livage and P. Judeinstein [29] and also Polleux et al. displayed comparable features of crystalline WO3 nanostructures [59]. From these FT-IR results, we can tell that heat treatment can play a significant effect on the adsorbed functional groups present on the thin film surface.

4.5 Wetting Properties

Investigation about the wettability of the surface was done by determining the angle of water on the (5^{th} -15^{th}) film layers calcined at 650 °C and the values got from the measurement can be seen in Table 1 and 2. The pure steel substrate θ average value measured was ascertained to be 100.07° which indicates the hydrophobic nature of the steel surface.

Table 2: The water contact angle (θ) values measured on the 5th layer W_Mo_O, W_O, and W_O(PVA) dip-coatings calcined at 650 °C (3 measurements executed from distinctive sites of the sample are labeled as 1st, 2nd, and 3rd).

Name:	**Contact angle (θ) (1^{st})**	**St. dev.**	**Contact angle (θ) (2^{nd})**	**St. dev.**	**Contact angle (θ) (3^{rd})**	**St. dev.**	**Average**
W Mo O	59.00	0.03	57.78	0.1	66.66	0.59	61.14
W_O	102.93	0.02	113.30	0.05	96.53	1.49	104.25
$W\_O_{(PVA)}$	69.49	0.01	56.44	0.08	67.25	0.68	64.39

Table 3: The water contact angle (θ) values measured on the 15th layer W_Mo_O, W_O, and W_O(PVA) dip-coatings calcined at 650 °C (3 measurements executed from distinctive sites of the sample are labeled as 1st, 2nd, and 3rd).

Name:	**Contact angle (θ) (1st)**	**St. dev.**	**Contact angle (θ) (2nd)**	**St. dev.**	**Contact angle (θ) (3rd)**	**St. dev.**	**Average**
W_Mo_O	30.90	0.68	23.00	0.05	22.75	0.10	25.55
W_O	100.94	0.03	96.44	0.65	95.09	0.37	97.49
$W\_O_{(PVA)}$	89.75	0.32	88.27	0.36	89.79	0.14	89.27

The grain boundaries and grooves present on the surface of the stainless steel (in Fig. 5) imply the simpler accretion of various organic-inorganic compounds when distinct liquid phases are in contact with it. In many instances, for the long-term build-up of unwanted materials, these deposits frequently serve as a preliminary material. The grooves and grain boundaries present on the steel surface were covered after the deposition of W_Mo_O & W_O films, and FE-SEM analysis confirmed that the topography adequately becomes smooth.

From the obtained θ results tell that when W_O (5^{th} film layer) is coated the θ value increased slightly while for the W_Mo_O film is decreased and the average values of θ were 61.14°, 104.25°, and 64.39°, for W_Mo_O, W_O, and $W\_O_{(PVA)}$ films, accordingly. The values of the WCA indicate that the 5^{th} layer of W_O film formed from the sol having a little amount of PVA act in hydrophobic nature, whereas $W\_O_{(PVA)}$ (with a larger amount of PVA) and W_Mo_O films produced with WCA<90° having hydrophilic properties.

When_θ value was measured on 15^{th} film layers, different results were attained (Table 2). For the W_O, average θ value was calculated to be 97.49 θ which slightly decreased, although for the $W\_O_{(PVA)}$ films displayed an increase in θ value by 24.88° (from 64.39° to 89.27°). Moreover, in comparing with the surface of the W_Mo_O 5^{th} film layer, the water contact angle for the 15^{th} layer W_Mo_O θ value decreased by 35° and surface were considerably lower whereas measurement of the contact angle on the $W\_O_{(PVA)}$ thin films ascent in the value of θ by 24.88° (i.e., from 64.39° to 89.27°). Observation shows the different behavior exhibited by the W_Mo_O film. Hydrophilic properties of the surface were indicated when the CA declined more from 61.14° to 25.55° degrees.

These contact angle values differences are assigned to the different grown films surface morphology and are sol composition dependent. The Metal ion concentration decreased when the PVA amount increased which leads to constraining the development of topographical structures on the surfaces. Nevertheless, the introduction of Mo ions in the WO3 matrix coatings provides evidence of hydrophilic character been produced. It is noted that the dip-coated films microstructures are complex and factors for example roughness, surface chemistry, homogeneity, and porosity contribute to the coating wettability. For example, the solid surface topographical effect on the wetting regime was discussed by Marmur [60] and surface porosity effects on the wetting anodized aluminum oxide (AAO) surfaces have been demonstrated by Buijnsters et al. [61]. When AAO structures that are highly porous were produced, an induced-structure conversion from slightly hydrophilic to moderately hydrophobic surfaces was presented by the authors and also they elaborated on the incident of hydrophobic wetting by penetration of water partially within the action of the capillary into the dead-end pore cavities along with a state of wetting in between the Cassie and Wenzel states [62]. Furthermore, the composition of the chemical describes the surface free energy and affects the wettability as a result [63,64]. This indicates that experimental analysis with surface variations that are different shall be executed presumably to approximate the actual wettability of any coating constructed in order to predict its character under large-scale applications. Selection of wet friction conditions was chosen for the tribological properties evaluation (of WO3 dip-coated thin films) and the thickness of the coats was understood clearly to be very low to resist a frictional from occurring exclusively of any lubricant between surfaces [35].

5. CONCLUSIONS AND RECOMMENDATIONS

Preparation of W_Mo_O, W_O, along with $W\_O_{(PVA)}$ films on the surface of stainless steel using an aqueous solution synthetic method was developed successfully. The films were deposited on a stainless steel substrate using the dip-coating technique and calcined (each coated layer) at 650 °C to become continuous as well as homogeneous.

It was seen from the temperature test results (in Fig. 3) that precursor gel decomposition, organic fragments, absorbed water molecules, and organic species are all eliminated gradually as temperature increases to 650 degree Celsius (gradually by 1 degree per minute) and also noted for the gels that the sintering-temperature of W_Mo_O was notably about 65 degree Celsius lesser than that of W_O, & $W\_O_{(PVA)}$ which can be due to the hydrophilic nature of W_Mo_O gel.

The FESEM analysis showed the spike-like topographical structures that were created on the surface of the oxide, depended on the concentration of the wetting agent, metal cation species as well as the number of layers dip-coated on the stainless steel substrate. Although all boundaries and holes were not fully cover after 15 coated thin film layers but showed the progress in a gradual reduction of the holes and boundaries size as the layer of coat increases.

Measurement of the WCA revealed that the hydrophobic and hydrophilic nature of WO3 films can be induced by the suggested chemical solution method through the alternation of solution parameters and the deposited number of layers on the steel substrate, while the WO3-Mo films that were formed by the same method had a hydrophilic nature. Probably the cost-effectiveness of the method proposed is also proved because of the simplicity of the used materials and processing conditions.

From the results obtained, even though it has improved the surface of the stainless steel greatly compare to its original state, it is openly understood that the layers coated are very thin to withstand greater effects of harms. The industrial application of this method can rest assured to have a good outcome and explore the full potential of WO3 films.

6. REFERENCES

[1] D. K. Tripathi, P. Ahmad, S. Sharma, D. K. Chauhan, and N. K. Dubey, Nanomaterials in Plants, Algae, and Microorganisms. 2017.

[2] H. Zheng, J. Z. Ou, M. S. Strano, R. B. Kaner, A. Mitchell, and K. Kalantar-Zadeh, "Nanostructured tungsten oxide - Properties, synthesis, and applications," Adv. Funct. Mater., 2011.

[3] M. Fernández-García, J.A. Rodriguez, Metal oxide nanoparticles, Encyclopedia of Inorganic Chemistry, John Wiley & Sons, Ltd, 2009, http://dx.doi.org/10.1002/ 0470862106.ia377.

[4] S. Pauliuk, R.L. Milford, D.B. Müller, J.M. Allwood, The steel scrap age, Environ. Sci. Technol. 47 (7) (2013) 3448.

[5] H. Mohrbacher, Reverse metallurgical engineering towards sustainable manufacturing of vehicles using Nb and Mo alloyed high performance steels, Adv. Manuf. 1 (1) (2013) 28.

[6] H.S. Link, R.J. Schmitt, Iron, carbon steel, and alloy steel. Materials of construction review, Ind. Eng. Chem. 53 (7) (1961) 590.

[7] V. Scotto, R.D. Cintio, G. Marcenaro, The influence of marine aerobic microbial film on stainless steel corrosion behaviour, Corros. Sci. 25 (3) (1985) 185.

[8] L. Chaves Simoes, M. Simoes, Biofilms in drinking water: problems and solutions, RSC Adv. 3 (8) (2013) 2520.

[9] M.F. Montemor, Functional and smart coatings for corrosion protection: a review of recent advances, Surf. Coat. Technol. 258 (2014) 17.

[10] M.J. Kreder, J. Alvarenga, P. Kim, J. Aizenberg, Design of anti-icing surfaces: smooth, textured or slippery? Nat. Rev. Mater. 1 (2016) 15003.

[11] N. Claudine, Polar oxide surfaces, J. Phys. Condens. Matter 12 (31) (2000) R367.

[12] S.K. Deb, Optical and photoelectric properties and colour centres in thin films of tungsten oxide, Philos. Mag. 27 (4) (1973) 801.

[13] N.M.G. Parreira, N.J.M. Carvalho, A. Cavaleiro, Synthesis, structural and mechanical characterization of sputtered tungsten oxide coatings, Thin Solid Films 510 (1) (2006) 191.

[14] J.M. Spurgeon, J.M. Velazquez, M.T. McDowell, Improving O2 production of WO3 photoanodes with IrO2 in acidic aqueous electrolyte, Phys. Chem. Chem. Phys. 16 (8) (2014) 3623.

[15] R.H. Coridan, M. Shaner, C. Wiggenhorn, B.S. Brunschwig, N.S. Lewis, Electrical and photoelectrochemical properties of WO3/Si tandem photoelectrodes, J. Phys. Chem. C 117 (14) (2013) 6949.

[16] P.K. Biswas, N.C. Pramanik, M.K. Mahapatra, D. Ganguli, J. Livage, Optical and electrochromic properties of sol–gel WO3 films on conducting glass, Mater. Lett. 57 (28) (2003) 4429.

[17] M. Sadakane, K. Sasaki, H. Kunioku, B. Ohtani, W. Ueda, R. Abe, Preparation of nano-structured crystalline tungsten (IV) oxide and enhanced photocatalytic activity for decomposition of organic compounds under visible light irradiation, Chem. Commun. (48) (2008) 6552.

[18] Y. Bai, T. Yang, Q. Gu, G. Cheng, R. Zheng, Shape control mechanism of cuprous oxide nanoparticles in aqueous colloidal solutions, Powder Technol. 227 (0) (2012) 35.

[19] D.B. Hernandez-Uresti, D. Sánchez-Martínez, A. Martínez-de la Cruz, S. Sepúlveda-Guzmán, L.M. Torres-Martínez, Characterization and photocatalytic properties of hexagonal and monoclinic WO3 prepared via microwave-assisted hydrothermal synthesis, Ceram. Int. 40 (3) (2014) 4767.

[20] A.B. Tesler, P. Kim, S. Kolle, C. Howell, O. Ahanotu, J. Aizenberg, Extremely durable biofouling-resistant metallic surfaces based on electrodeposited nanoporous tungstite films on steel, Nat. Commun. 6 (2015) 8649.

[21] C.C. Mardare, A.W. Hassel, Investigations on bactericidal properties of molybdenum–tungsten oxides combinatorial thin film material libraries, ACS Comb. Sci. 16 (11) (2014) 631.

[22] Y.J. Oh, M. Hubauer-Brenner, P. Hinterdorfer, Influence of surface morphology on the antimicrobial effect of transition metal oxides in polymer surface, J. Nanosci. Nanotechnol. 15 (10) (2015) 7853.

[23] G. Azimi, R. Dhiman, H.-M. Kwon, A.T. Paxson, K.K. Varanasi, Hydrophobicity of rare-earth oxide ceramics, Nat. Mater. 12 (4) (2013) 315.

[24] J. Drzymala, Hydrophobicity and collectorless flotation of inorganic materials, Adv. Colloid Interf. Sci. 50 (1994) 143.

[25] V.D. Ta, A. Dunn, T.J. Wasley, J. Li, R.W. Kay, J. Stringer, P.J. Smith, E. Esenturk, C. Connaughton, J.D. Shephard, Laser textured superhydrophobic surfaces and their applications for homogeneous spot deposition, Appl. Surf. Sci. 365 (2016) 153.

[26] C. Gu, J. Zhang, J. Tu, A strategy of fast reversible wettability changes of WO3 surfaces between superhydrophilicity and superhydrophobicity, J. Colloid Interface Sci. 352 (2) (2010) 573.

[27] A. Nakajima, Design of hydrophobic surfaces for liquid droplet control, NPG Asia Mater. 3 (2011) 49.

[28] M. Shaban, M. Zayed, H. Hamdy, Nanostructured ZnO thin films for self-cleaning applications, RSC Adv. 7 (2) (2017) 617.

[29] P. Judeinstein, J. Livage, Sol-gel synthesis of WO3 thin films, J. Mater. Chem. 1 (4) (1991) 621.

[30] V. Cristino, S. Caramori, R. Argazzi, L. Meda, G.L. Marra, C.A. Bignozzi, Efficient photoelectrochemical water splitting by anodically grown WO3 electrodes, Langmuir 27 (11) (2011) 7276.

[31] P. Tägtström, U. Jansson, Chemical vapour deposition of epitaxial WO3 films, Thin Solid Films 352 (1) (1999) 107.

[32] Y.S. Zou, Y.C. Zhang, D. Lou, H.P. Wang, L. Gu, Y.H. Dong, K. Dou, X.F. Song, H.B. Zeng, Structural and optical properties of WO3 films deposited by pulsed laser deposition, J. Alloys Compd. 583 (2014) 465.

[33] E. Garskaite, M. Lindgren, M.-A. Einarsrud, T. Grande, Luminescent properties of rare earth (Er, Yb) doped yttrium aluminium garnet thin films and bulk samples synthesised by an aqueous sol–gel technique, J. Eur. Ceram. Soc. 30 (7) (2010) 1707.

[34] T.O.L. Sunde, E. Garskaite, B. Otter, H.E. Fossheim, R. Saeterli, R. Holmestad, M.- A. Einarsrud, T. Grande, Transparent and conducting ITO thin films by spin coating of an aqueous precursor solution, J. Mater. Chem. 22 (31) (2012) 15740.

[35] J. Raudoniene, A. Laurikenas, M.M. Kaba, G. Sahin, A.U. Morkan, D. Brazinskiene, S. Asadauskas, R. Seidu, A. Kareiva, E. Garskaite, Textured WO3 and WO3:Mo films deposited from chemical solution on stainless steel, Thin Solid Films 653 (2018) 179–187.

[36] C.J. Brinker, A.J. Hurd, "Fundamentals of sol-gel dip-coating", J. Phys. III France 4 (1994) 1231-1242

[37] A. Mahmood and A. Naeem, "Sol-Gel-Derived Doped ZnO Thin Films: Processing, Properties, and Applications," in Recent Applications in Sol-Gel Synthesis, 2017.

[38] V. Himaja, S. K. O, R. Karthikeyan, and S. B. P, "A Comprehensive Review on Tablet Coating," Austin Pharmacol. Pharm., vol. 1, no. 1, pp. 1–8, 2016.

[39] C.V. Ramana, S. Utsunomiya, R.C. Ewing, C.M. Julien, U. Becker, Structural stability and phase transitions in WO3 thin films, J. Phys. Chem. B 110 (21) (2006) 10430.

[40] P.M. Woodward, A.W. Sleight, T. Vogt, Ferroelectric tungsten trioxide, J. Solid State Chem. 131 (1) (1997) 9.

[41] T. Vogt, P.M. Woodward, B.A. Hunter, The high-temperature phases of WO3, J. Solid State Chem. 144 (1) (1999) 209.

[42] T. Liu, J. Liu, Q. Hao, Q. Liu, X. Jing, H. Zhang, G. Huang, J. Wang, Porous tungsten trioxide nanolamellae with uniform structures for high-performance ethanol sensing, CrystEngComm 18 (43) (2016) 8411.

[43] S. Bai, K. Zhang, X. Shu, S. Chen, R. Luo, D. Li, A. Chen, Carboxyl-directed hydrothermal synthesis of WO3 nanostructures and their morphology-dependent gassensing properties, CrystEngComm 16 (44) (2014) 10210.

[44] S.-H. Kim, H. Kim, N.J. Kim, Brittle intermetallic compound makes ultrastrong lowdensity steel with large ductility, Nature 518 (7537) (2015) 77.

[45] S. Pokhrel, J. Birkenstock, M. Schowalter, A. Rosenauer, L. Mädler, Growth of ultrafine single crystalline WO3 nanoparticles using flame spray pyrolysis, Cryst. Growth Des. 10 (2) (2010) 632.

[46] K.R. Reyes-Gil, C. Wiggenhorn, B.S. Brunschwig, N.S. Lewis, Comparison between the quantum yields of compact and porous WO3 photoanodes, J. Phys. Chem. C 117 (29) (2013) 14947.

[47] J.H. Christopher, L. Vittorio, S.K. Kevin, High-temperature phase transitions in tungsten trioxide - the last word? J. Phys. Condens. Matter 14 (3) (2002) 377.

[48] C. Santato, M. Odziemkowski, M. Ulmann, J. Augustynski, Crystallographically oriented mesoporous WO3 films: synthesis, characterization, and applications, J. Am. Chem. Soc. 123 (43) (2001) 10639.

[49] Q. Mi, Y. Ping, Y. Li, B. Cao, B.S. Brunschwig, P.G. Khalifah, G.A. Galli, H.B. Gray, N.S. Lewis, Thermally stable N2-intercalated WO3 photoanodes for water oxidation, J. Am. Chem. Soc. 134 (44) (2012) 18318.

[50] N. Sharma, M. Deepa, P. Varshney, S.A. Agnihotry, FTIR investigations of tungsten oxide electrochromic films derived from organically modified peroxotungstic acid precursors, Thin Solid Films 401 (1) (2001) 45.

[51] S.W. Bruun, A. Kohler, I. Adt, G.D. Sockalingum, M. Manfait, H. Martens, Correcting attenuated total reflection—Fourier transform infrared spectra for water vapor and carbon dioxide, Appl. Spectrosc. 60 (9) (2006) 1029.

[52] T. Schadle, B. Pejcic, B. Mizaikoff, Monitoring dissolved carbon dioxide and methane in brine environments at high pressure using IR-ATR spectroscopy, Anal. Methods 8 (4) (2016) 756.

[53] M.K. Bernett, W.A. Zisman, Effect of adsorbed water on the critical surface tension of wetting on metal surfaces, J. Colloid Interface Sci. 28 (2) (1968) 243.

[54] M.M. Gentleman, J.A. Ruud, Role of hydroxyls in oxide wettability, Langmuir 26 (3) (2010) 1408.

[55] H. Tamura, K. Mita, A. Tanaka, M. Ito, Mechanism of hydroxylation of metal oxide surfaces, J. Colloid Interface Sci. 243 (1) (2001) 202.

[56] E.J. Baran, C.C. Wagner, M.H. Torre, Synthesis and characterization of EDTA complexes useful for trace elements supplementation, J. Braz. Chem. Soc. 13 (2002) 576.

[57] M.F.G. Esteban, R.V. Serrano, F.G. Vilchez, Synthesis and vibrational study of some polydentate ligands, Spectrochim. Acta A. 43 (8) (1987) 1039.

[58] J.P. Devlin, J. Sadlej, V. Buch, Infrared spectra of large H2O clusters: new understanding of the elusive bending mode of ice, J. Phys. Chem. A 105 (6) (2001) 974.

[59] J. Polleux, N. Pinna, M. Antonietti, M. Niederberger, Growth and assembly of crystalline tungsten oxide nanostructures assisted by bioligation, J. Am. Chem. Soc. 127 (44) (2005) 15595.

[60] A. Marmur, Wetting on hydrophobic rough surfaces: to be heterogeneous or not to be? Langmuir 19 (20) (2003) 8343.

[61] J.G. Buijnsters, R. Zhong, N. Tsyntsaru, J.-P. Celis, Surface wettability of macroporous anodized aluminum oxide, ACS Appl. Mater. Interfaces 5 (8) (2013) 3224.

[62] A.M.A. Mohamed, A.M. Abdullah, N.A. Younan, Corrosion behavior of superhydrophobic surfaces: a review, Arab. J. Chem. 8 (6) (2015) 749.

[63] A. Bondi, The spreading of liquid metals on solid surfaces. Surface chemistry of high-energy substances, Chem. Rev. 52 (2) (1953) 417.

[64] W. Toshiya, Wettability of ceramic surfaces - a wide range control of surface wettability from super hydrophilicity to super hydrophobicity, from static wettability to dynamic wettability, J. Ceram. Soc. Jpn. 117 (2009) 1285.

7. APPENDICES

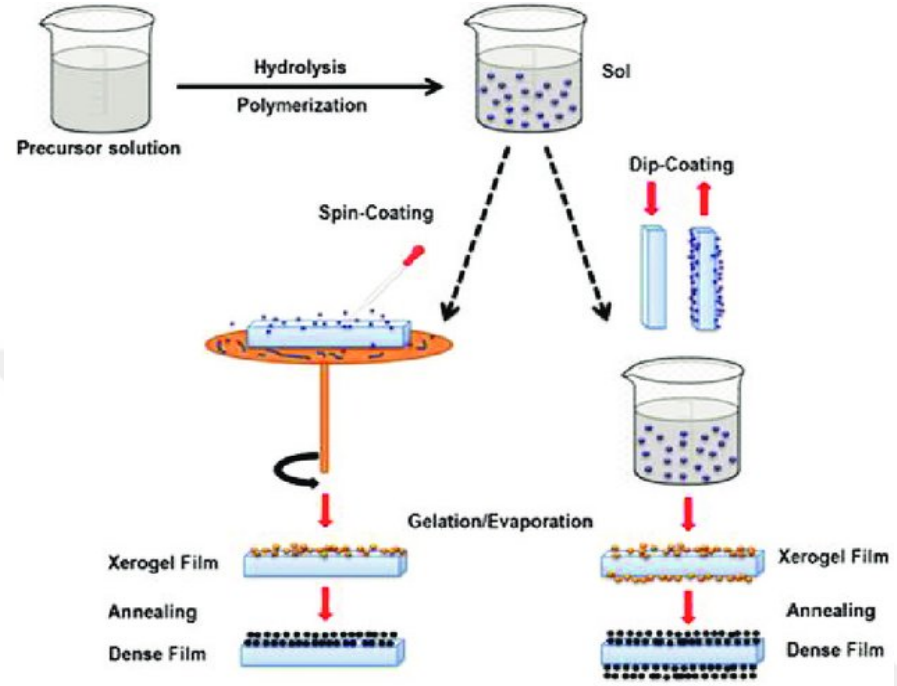

Fig. 1: Diagram briefly showing the sol-gel and thin film processing [37].

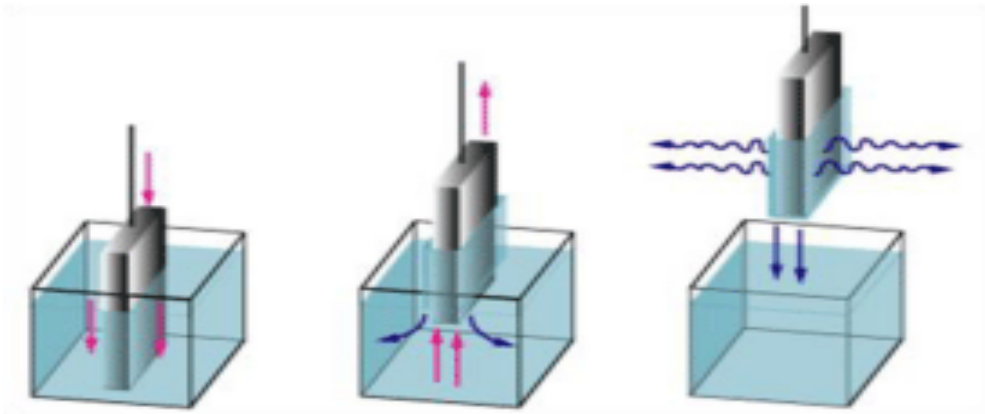

Fig. 2: Dip-coating process [38].

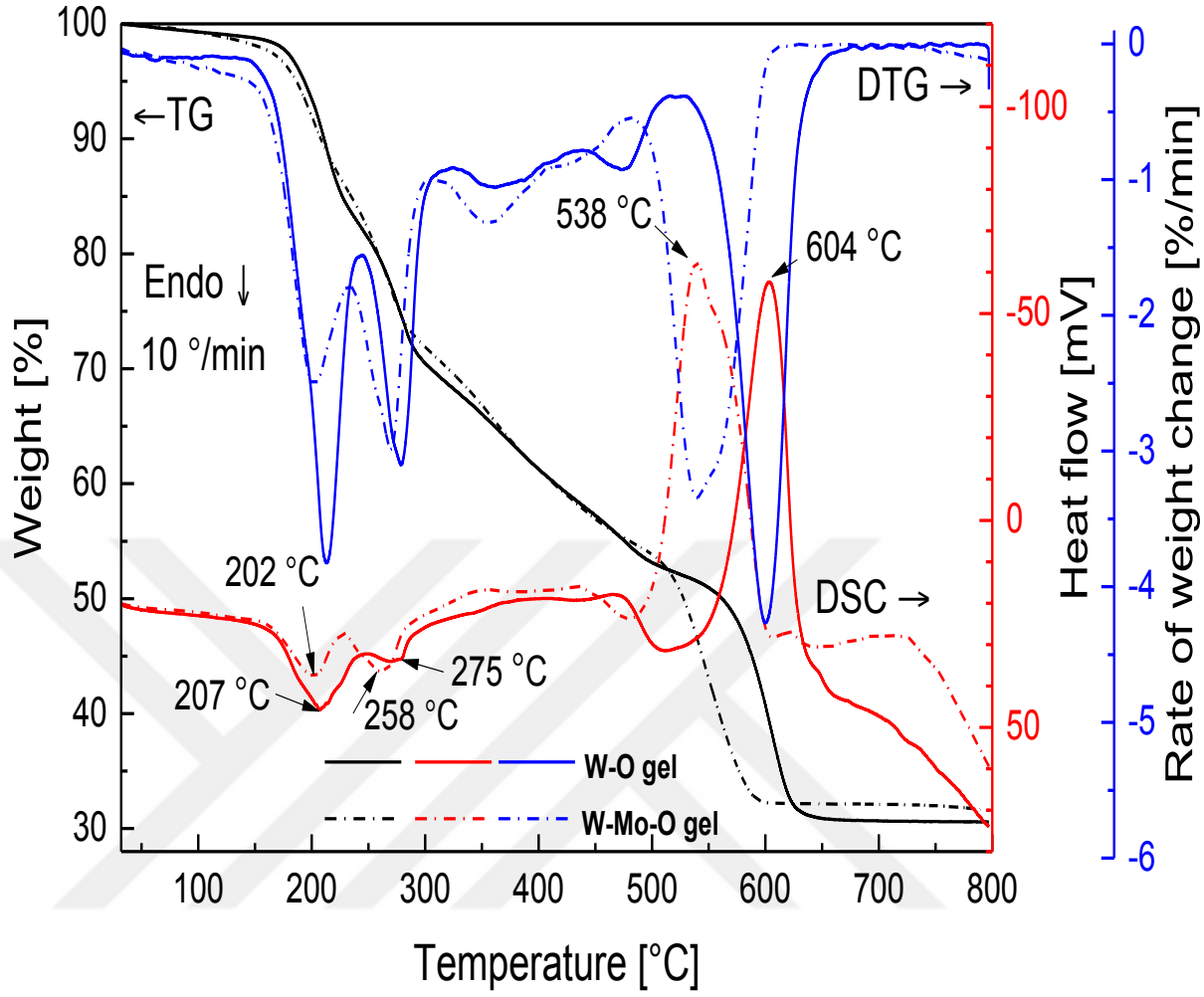

Fig.3: The DTG and TG/DSC curves of W_Mo_O along with W_O gels.

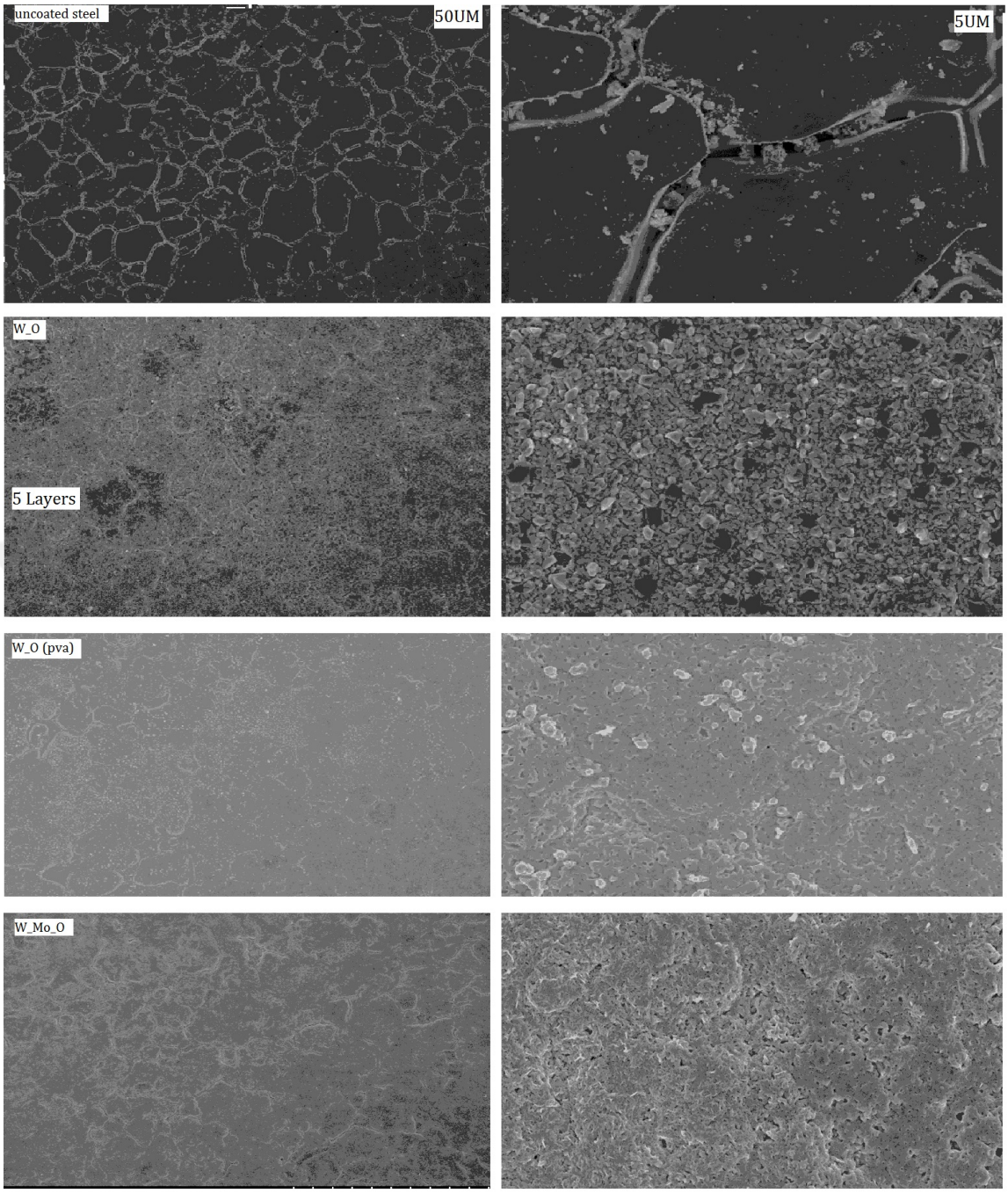

Fig.4: Five & Fifty micrometers SEM images (of the 5th layer) from the smallest boundaries of the steel along with uncoated steel.

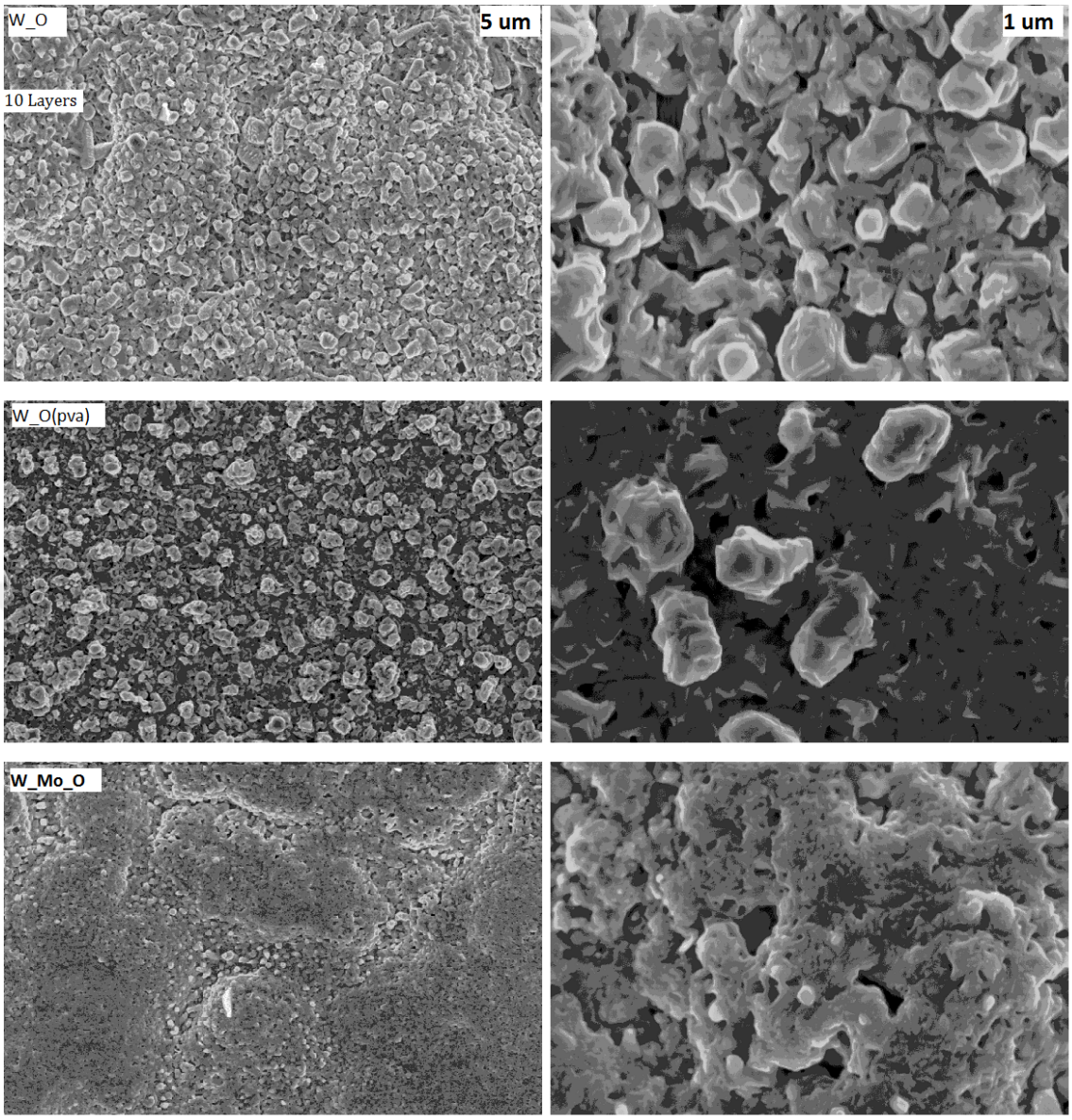

Fig.5: The five & one micrometers SEM images of the 10th coated film layers.

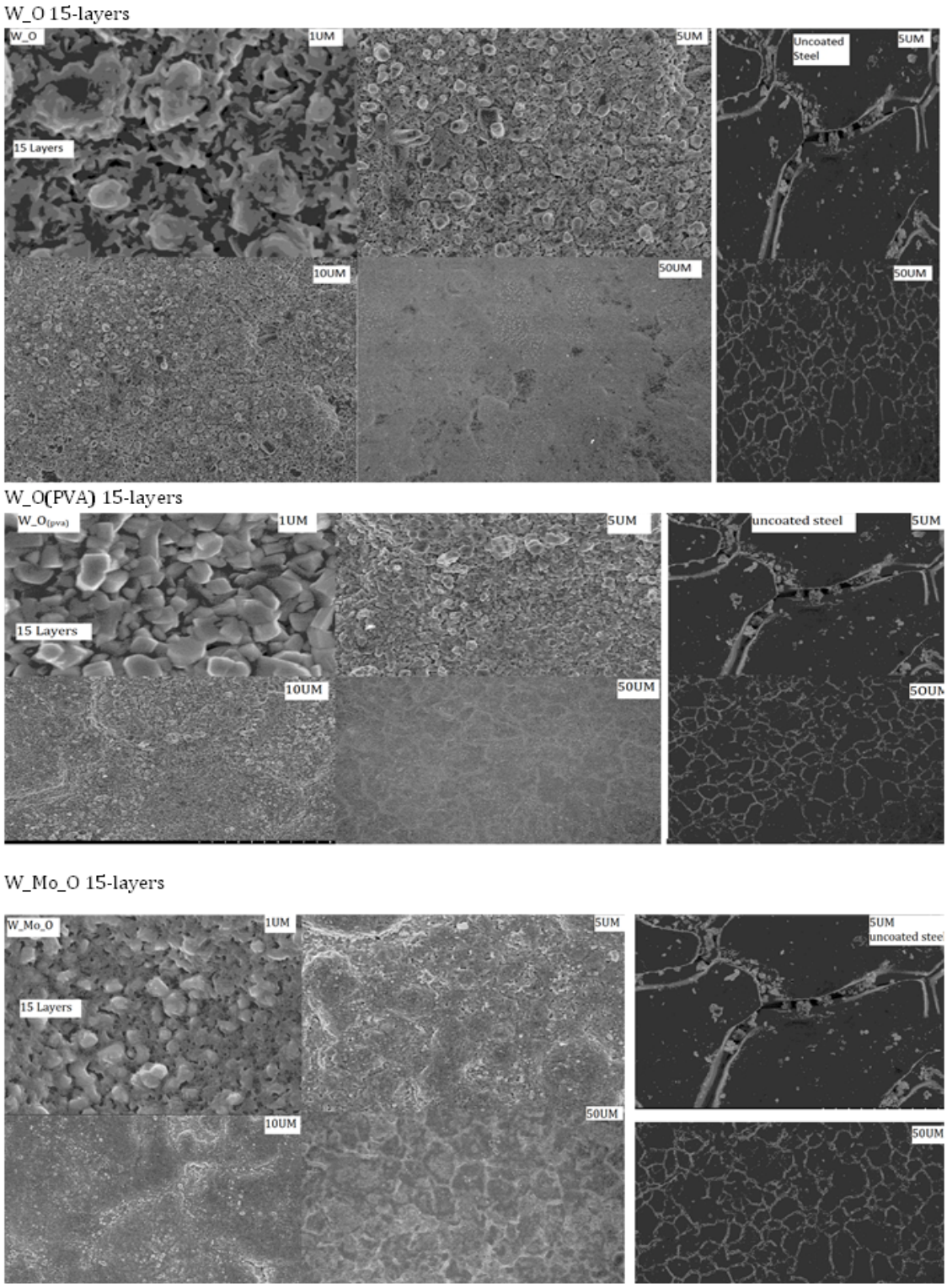

Fig.6: SEM images of 15th coated layers (from all samples) compared with uncoated steel in various micrometers.

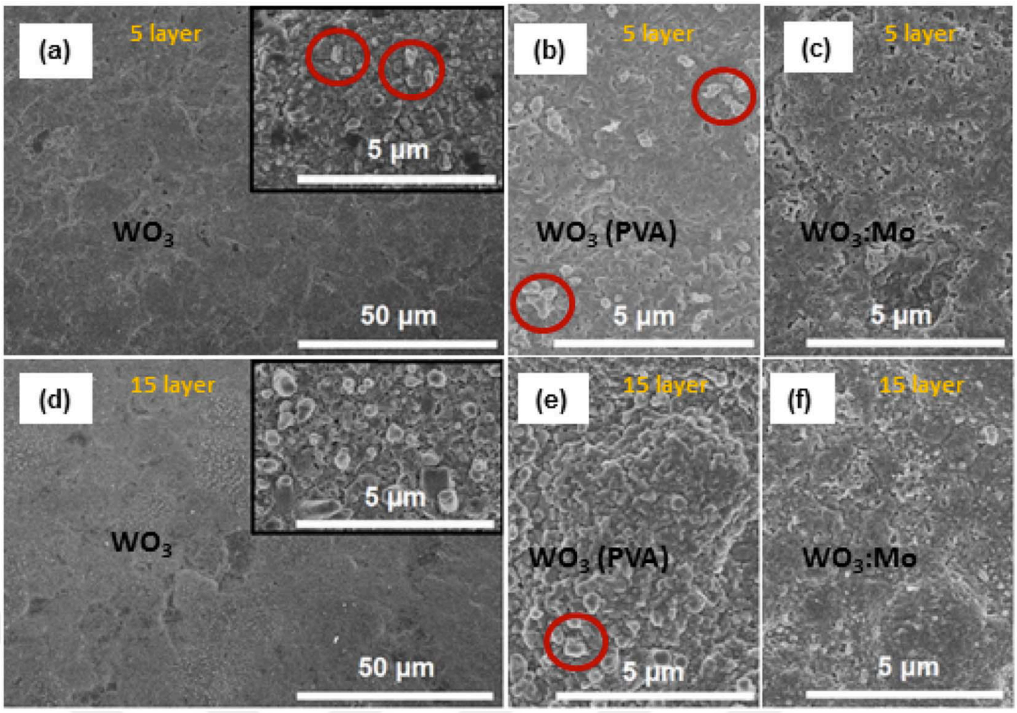

Fig. 7: FE-SEM micrographical images of the 5th & 15th layer ((a), (d)) W_O, ((b), (e)) W_$O_{(PVA)}$ & ((c), (f)) W_Mo_O films calcined for 5 h at 650 °C .

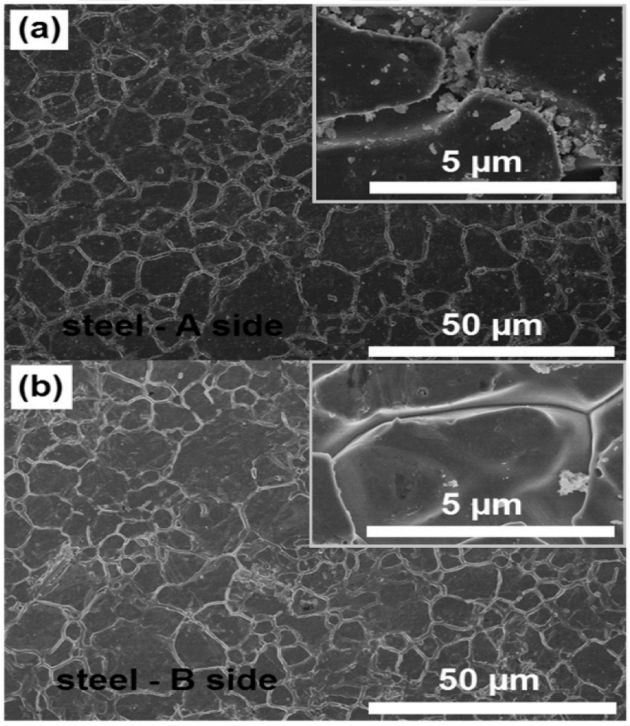

Fig. 8: FE-SEM micrographic images of the stainless steel substrate (a) upper-surface (A-side) and (b) lower-surface (B-side) (films produced on the upper-surface were examined).

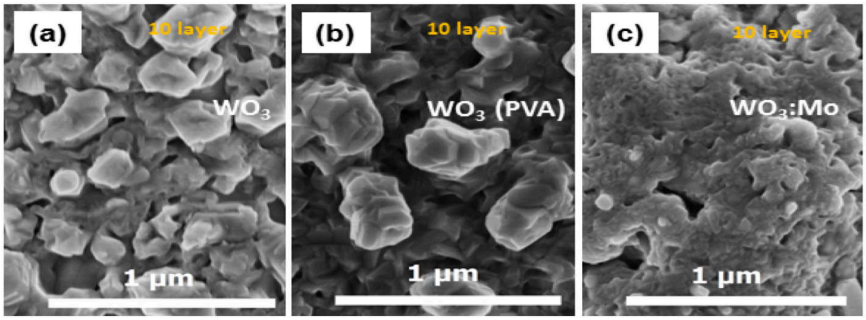

Fig. 9: Fig. 9: FE-SEM micrographic images of 10th layer (a) W_O, (b) W_O(PVA) & (c) W_Mo_O films calcined at 650 °C for 5 h

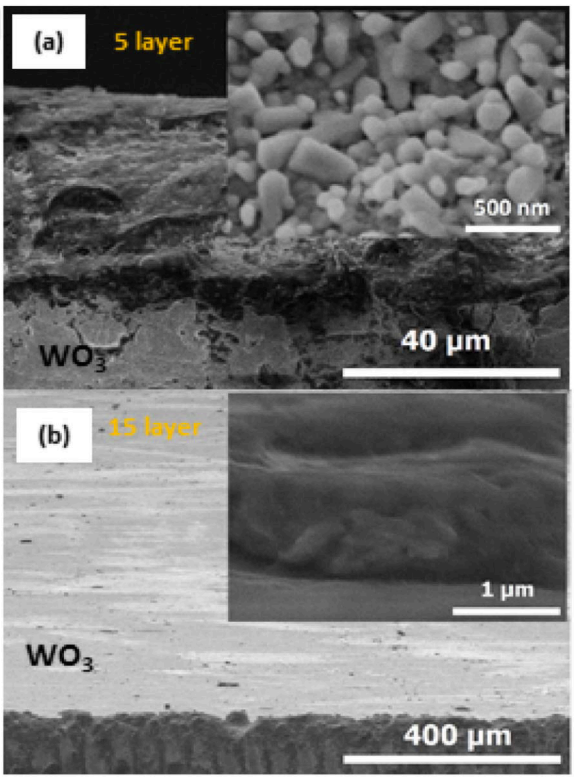

Fig. 10: Cross-sectional FE-SEM micrographic images of (a) 5th layer & (b) 15th layer W_O films calcined at 650 °C for 5 h; (a) inset shows the polycrystalline film microstructure and (b) inset presents W_O film from the coating center.

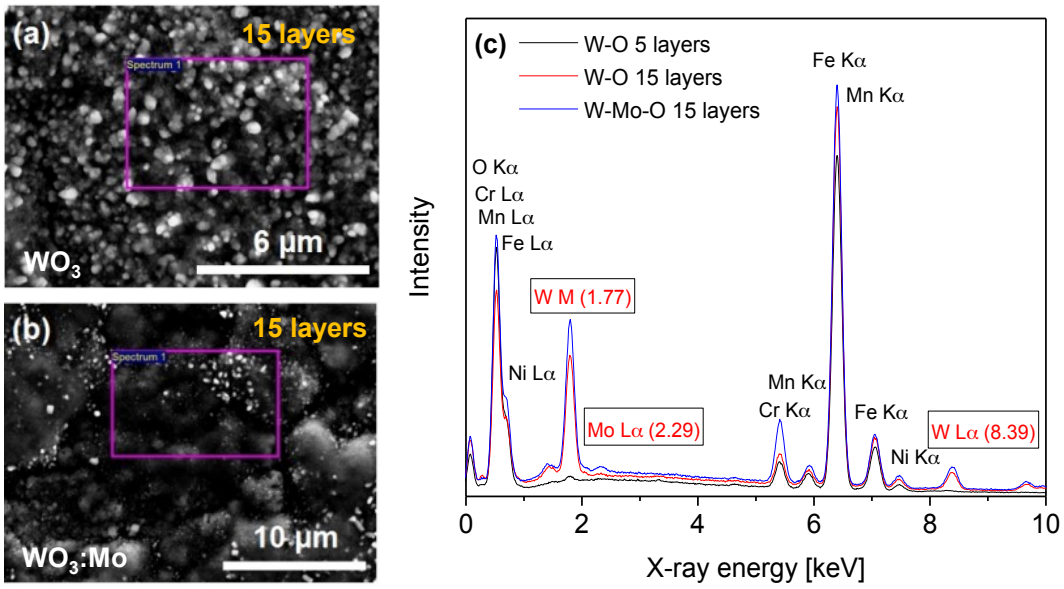

Fig. 11: FE-SEM micrographic images (places marked indicate the surface region scanned) along with the EDS spectrum of W_O & W_Mo_O films.

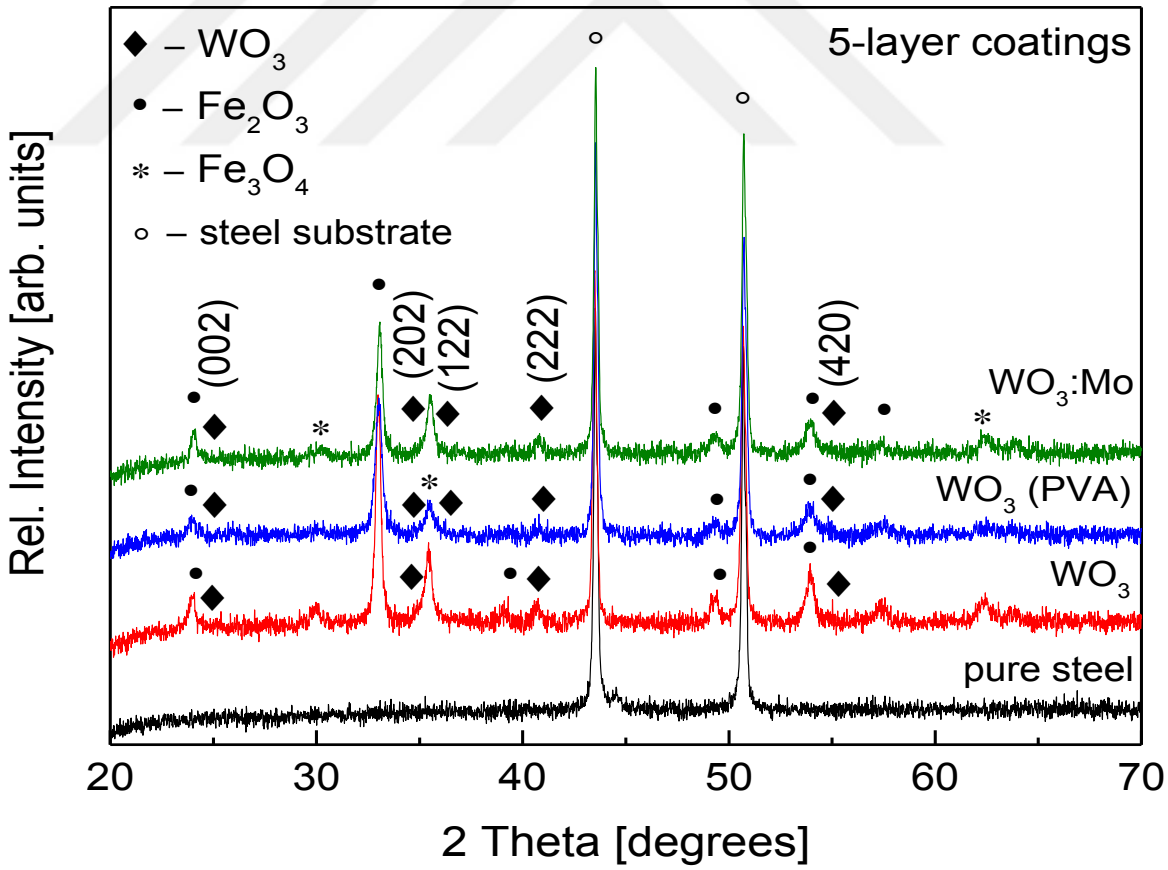

Fig. 12: The XRD patterns of the 5th coated layer of W_Mo_O, W_O, & W_O$_{(PVA)}$ as well as the pure uncoated steel substrate calcined for 5 h at 650 °C.

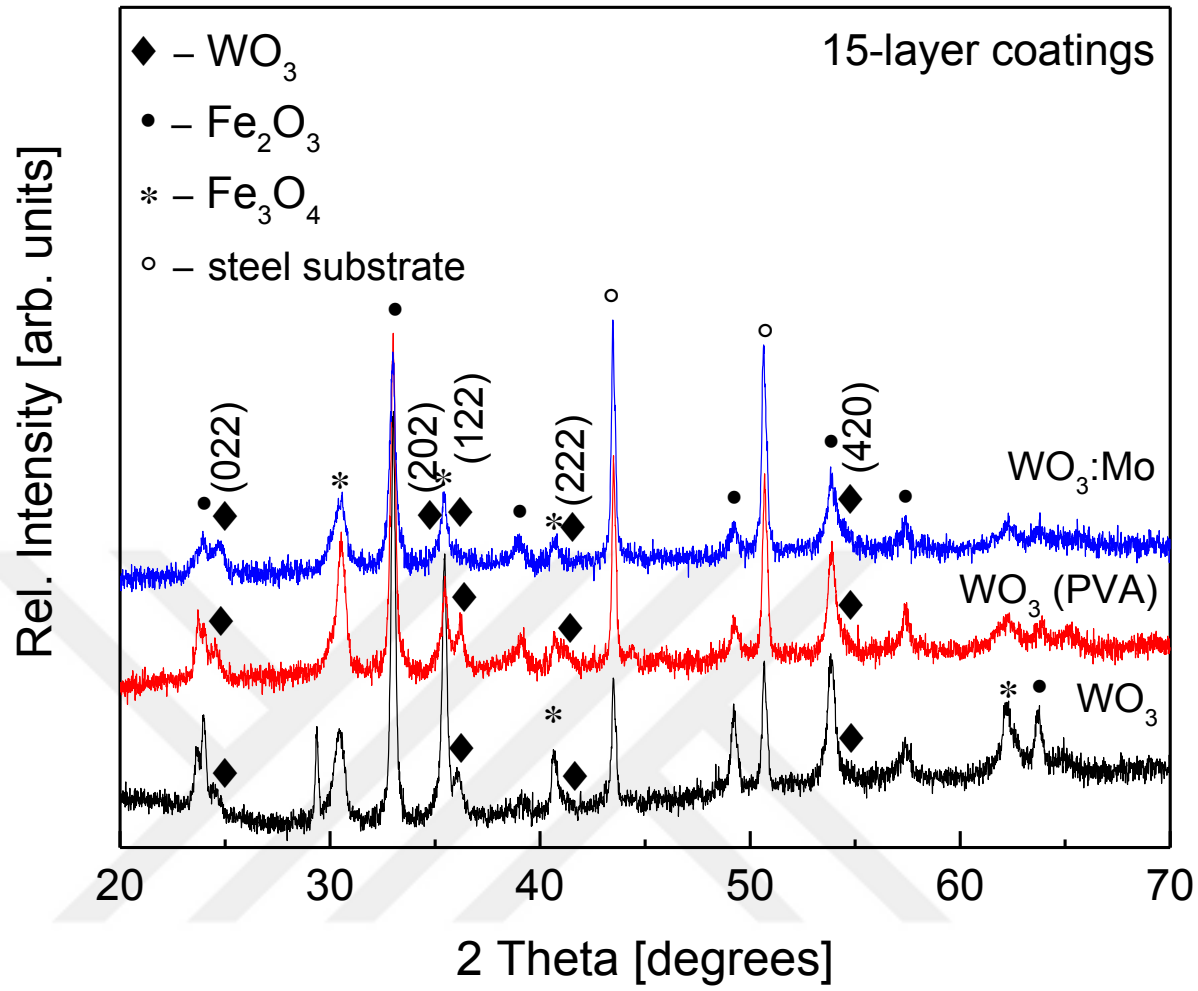

Fig. 13: XRD patterns of pure steel substrate and 15th layer W_Mo_O, W_O along with W_$O_{(PVA)}$ coatings calcined for 5 h at 650 °C.

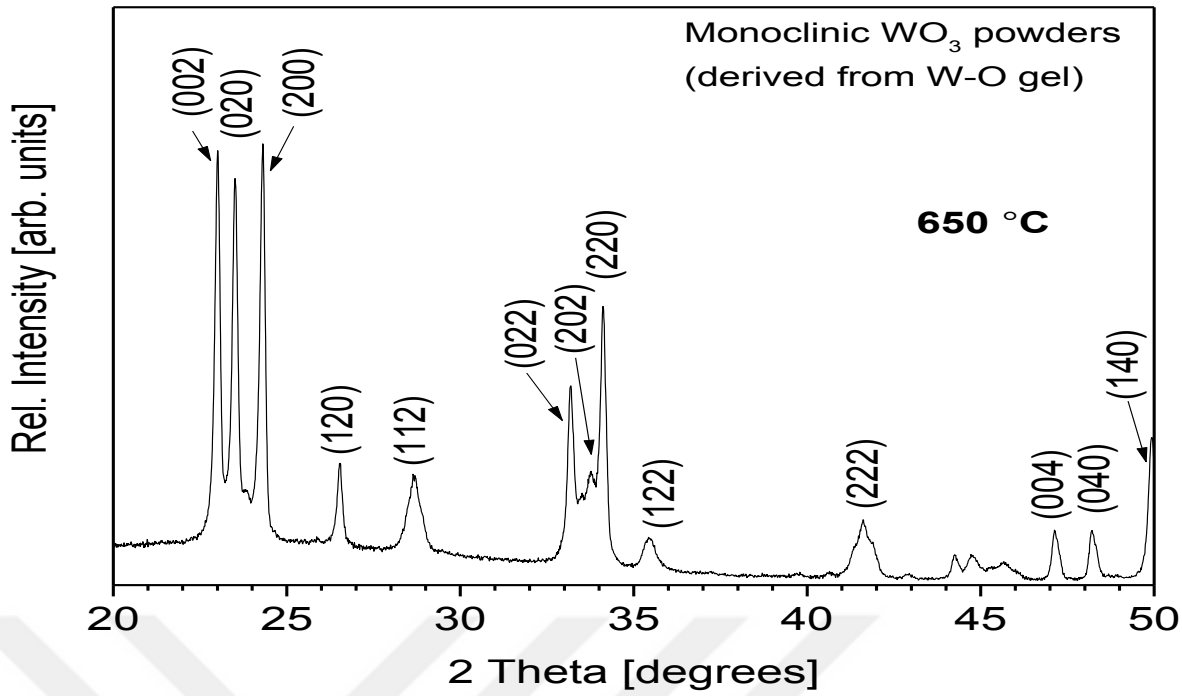

Fig. 14: W_O gel powders XRD diffraction pattern calcined at 650 °C displaying the crystalline monoclinic WO3 formation.

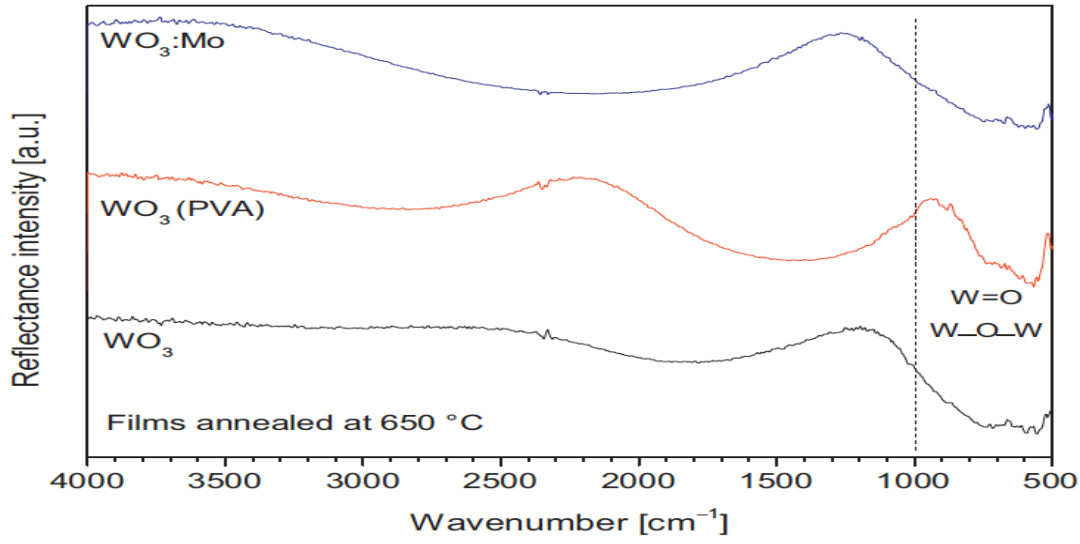

Fig. 15. FT-IR spectra of the 15th coated film layer of W_Mo_O, W_O, along with $W\_O_{(PVA)}$ coatings calcined at 650 °C.

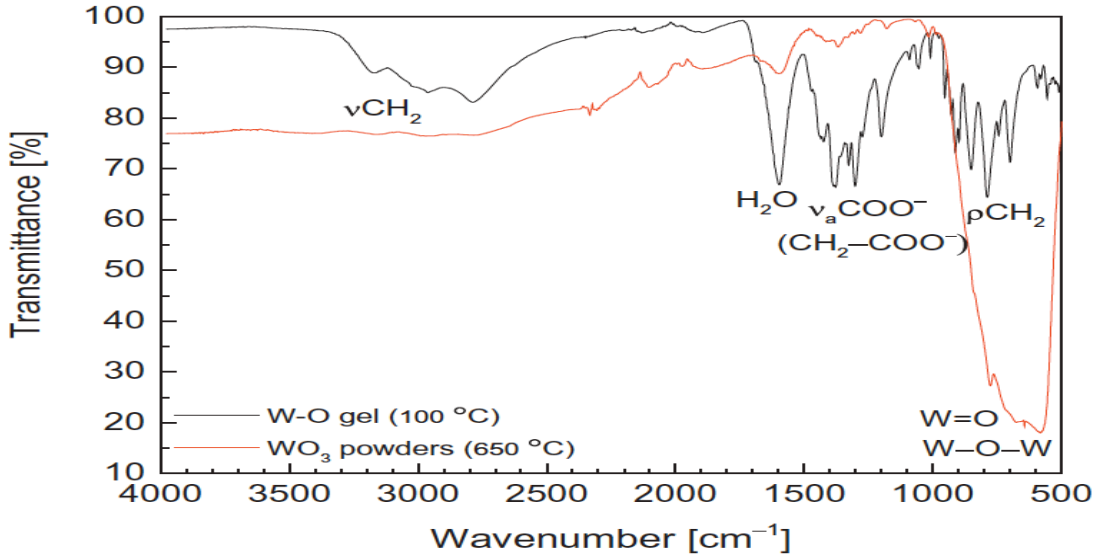

Fig. 16. FT-IR spectra analysis of the WO3 powders calcined at 650 °C and W-O gel dried at 100 °C.

8. CURRICULUM VITAE

EDUCATION AND TRAINING	Date
Bachelor of Science: Chemistry Abant Izzet Baysal University Bolu, Turkey.	31/10/2012– 19/06/2017
Diploma in Computer software programs Inter Digital Computer School Mechlin Street, Monrovia, Liberia.	01/07/2012– 10/10/2012
Secondary Education Diploma Muslim Congress High School Mechlin Street, Monrovia, Liberia.	01/09/1998– 30/06/2012
Biochemistry, Pharmacology, Genetics, and Microbiology Internship Laboratory works in: Pharmacology, Genetics, Biochemistry, and Microbiology. Learned basic cell culture techniques, elisa reader applications, clinical microbiological, and gene sequencing techniques. Faculty of Medicine, Abant Izzet Baysal University, Bolu, Turkey.	05/07/2015– 06/08/2015
Certificate of Education WAS (World Accredited Services) Youngs of Today and Leaders of Tomorrow; Leadership and Time Management with NLP. Abant Izzet Baysal University, Bolu, Turkey.	08/03/2014– 10/03/2014

Certificate of Education 01/11/2010–

AISEC Liberia, workshop-training program 01/12/2010

The AISEC workshop-training program helps me to learn more about harmful diseases, and how to save oneself and society from such diseases (Mainly talked about HIV / AIDS).

Monrovia, Liberia.

WORK EXPERIENCE

Chemist

MNG Gold Liberia Inc.

09/09/2019–
Present

Analysis of the amount of gold in solid & liquid samples, determining the chemical content of the waste products, & also serving as an English-Turkish Translator between the Liberians and Turkish workers.

Kokoya District, Bong County, Liberia.

Chemist

Cevahir Leather Factory

4/09/2017–
05/12/2018

Mixing of chemicals in the leather laboratory, & also served as an English-Turkish Translator.

Tuzla, Istanbul, Turkey

Language School Teacher

Ideal Team Academy 07/08/2014–

English School Teacher for elementary, junior, and senior high school students. 10/11/2015

Bolu/Düzce, Turkey.

AWARDS

Certificate of honor (ASUB*)*

For hard work in establishing ASUB (African Student Association in Bolu), 13/05/2017

Abant İzzet Baysal, University, Bolu, Turkey.

Most Improve student

Muslim Congress high school, 20/04/2011

Mechlin Street, Monrovia, Liberia.

Certificate of honor General Secretary

Dawah school club, Muslim Congress High school,

Mechlin Street, Monrovia, Liberia 30/06/2012

June 30, 2012

LIST OF PUBLICATIONS

Authors: J. Raudoniene, A. Laurikenas, M.M. Kaba, G. Sahin, A.U. Morkan, D. Brazinskiene, S. Asadauskas, R. Seidu, A. Kareiva, E. Garskaite. 15/03/2018

Article: Textured WO3 and WO3: Mo films deposited from chemical solution on stainless steel, Thin Solid Films 653 (2018) 179–187.

Authors: Smalenskaite,M. M. Kaba, I. Grigoraviciute-Puroniene,1 L. Mikoliunaite, A. Zarkov,1 R. Ramanauskas, I. A. Morkan, and A. Kareiva. 12/11/2019

Article: Sol-Gel Synthesis and Characterization of Coatings of Mg-Al Layered Double Hydroxides, Materials (Basel). 2019 Nov; 12(22): 3738.

9. ORIGANILITY REPORT

T.R.
BOLU ABANT İZZET BAYSAL UNIVERSITY
DIRECTORATE OF INSTITUTE OF GRADUATE STUDIES

STUDENT & SUPERVISOR PLAGIARISM DECLARATION FORM

Department	Chemistry
Name and surname	Musa Mohammed KABA
Student number	17161040104
Postgraduate program	MSc with thesis ✓ PhD ☐
Academic year and semester of thesis examination	2020 / 2021 Autumn ✓ Spring ☐
Thesis defence date	06-01-2021
Number of pages	63
Thesis title (Tr)	PASLANMAZ ÇELIK ÜZERINE DALDIRMA YOLUYLA TUNGSTEN TROKST KAPLAMA
Thesis title (Eng)	DIP COATING OF TUNGSTEN TRIOXIDE ON A STAINLESS STEEL

Based on the plagiarism report that was generated on the date of ____/01/2021 by using predetermined filtrations set by Directorate of Institute of Graduate Studies of the Turnitin programme, a plagiarism detection sofware, the rate of plagiarism detected was 25 %.

We hereby declare that this thesis does not consist any kind of plagiarism, that the information we have given above is correct, and accept all kinds of legal liability in case of any contradiction otherwise.

Musa Mohammed KABA
Student
(Name, Surname, date ve Signature)

Prof. Dr. Izzet MORKAN
Supervisor
(Name, Surname, date ve Signature)

Instructions:

1. After the thesis defense exam with success, a similarity index (plagiarism) report is obtained once again by using the final version of thesis dissertation file containing all the possible changes, and the rate (%) of plagiarism is entered in the "Student & Supervisor Plagiarism Declaration Form".
2. Following the defance exam, this form must be prepared by the student **electronically** and submitted to the Institute via the head of related department by the thesis supervisor in order to be kept in the student file together with the "thesis submission form (*after the thesis defence exam version*)".

11b- İntihal beyan formu

T.C.
BOLU ABANT İZZET BAYSAL ÜNİVERSİTESİ
LİSANSÜSTÜ EĞİTİM ENSTİTÜSÜ MÜDÜRLÜĞÜ

ÖĞRENCİ ve TEZ DANIŞMANI İNTİHAL BEYAN FORMU

Anabilim Dalı	Kimya		
Öğrencinin Adı ve Soyadı	Musa Mohammed KABA		
Numarası	17161040104		
Lisansüstü Programı	Tezli Yüksek Lisans ☑	Doktora ☐	
Tez Sınavına Girdiği Eğitim Yılı ve Dönemi	2020 / 2021	☑ Güz	☐ Bahar
Tez Sınavına Girdiği Tarih	06-01-2021		
Tezin Sayfa Sayısı	63		
Tez Başlığı (Tr)	PASLANMAZ ÇELİK ÜZERİNE DALDIRMA YOLUYLA TUNGSTEN TRIOKSİT KAPLAMA		
Tez Başlığı (En)	DIP COATING OF TUNGSTEN TRIOXIDE ON A STAINLESS STEEL		

Teze ilişkin ____/01/2021 tarihinde yapılan Turnitin adlı intihal tespit programından enstitü müdürlüğünce belirlenen filtrelemeler uygulanarak alınmış olan benzerlik raporuna göre, tezin benzerlik oranı % 25 olarak tespit edilmiştir.

Bu tez çalışmasının herhangi bir intihal içermediğini; aksinin tespit edilmesi durumunda doğabilecek her türlü hukuki sorumluluğu kabul ettiğimizi ve yukarıda vermiş olduğumuz bilgilerin doğru olduğunu beyan ederiz.

Musa Mohammed KABA
Öğrenci
(Adı, Soyadı, tarih ve İmza)

Prof. Dr. İzzet MORKAN
Tez Danışmanı Onayı
(Adı, soyadı, tarih ve İmza)

Açıklamalar:
1-Tez savunma sınavı sonrasında başarılı bulunan öğrencinin tez çalışması muhtemel değişiklikleri içeren dosya halinde/cd ortamında ikinci bir benzerlik raporu alınır. "Öğrenci ve Tez Danışmanı İntihal Beyan Formu"na işlenir.
*2- Bu form öğrenci tarafından **elektronik ortamda** hazırlandıktan ve tez sınavından sonra "tez teslim formu (tez sınavı sonrası)" ile birlikte öğrenci dosyasında saklanmak üzere tez danışmanı tarafından EABİS otomasyon sistemine yüklenmelidir.*